Pre-clinical cancer studies:

mTOR signalling mechanisms as a therapeutic target

Student: David Keith Hunt

Supervisor: Dr. Andrew Robert Tee

Co-Supervisor: Prof. Julian Sampson

Student Number: 0520982

DECLARATION

This work has not previously been accepted in substance for any degree and is not concurrently submitted in candidature for any degree.

Signed …… (candidate) Date ……

STATEMENT 1

This thesis is being submitted in partial fulfillment of the requirements for the degree of MPhil.

Signed …… (candidate) Date ……

STATEMENT 2

This thesis is the result of my own independent work/investigation, except where otherwise stated. Other sources are acknowledged by explicit references.

Signed …… (candidate) Date ……

STATEMENT 3

I hereby give consent for my thesis, if accepted, to be available for photocopying and for inter-library loan, and for the title and summary to be made available to outside organisations.

Signed …… (candidate) Date ……

STATEMENT 4: PREVIOUSLY APPROVED BAR ON ACCESS

I hereby give consent for my thesis, if accepted, to be available for photocopying and for inter-library loans **after expiry of a bar on access previously approved by the Graduate Development Committee.**

Signed …… (candidate) Date ……

Contents

Table of Figures

Summary

Defects in mechanistic Target of Rapamycin Complex 1 (mTORC1) signalling are the cause of a number of heritable human diseases such as Tuberous Sclerosis Complex, Neurofibromatosis and Birt-Hogg-Dubé syndrome. Mutations in signalling components in the mTORC1 signalling pathway are also present in a significant number of sporadic cancers, such as bladder and renal cancer. A number of mTORC1-driven features arise as a result of these mutations that offer opportunities to develop selective therapeutic strategies that exploit such differences. One such variation that has been suggested is that cells with upregulated mTORC1 activity have elevated levels of Endoplasmic Reticulum (ER) stress. The clinically approved HIV protease inhibitor, Nelfinavir, has been suggested to exacerbate ER stress. The aim of this project was to examine whether Nelfinavir could be used to exploit existing basal elevations in ER stress in cells with aberrant mTORC1 signalling to selectively induce cell death. In addition to assessing the therapeutic potential of this drug treatment strategy, this project sought to further examine interactions between mTORC1 signalling and autophagy, a major survival component of the ER stress response. The results of experimentation demonstrated the increased susceptibility of TSC deficient cells to ER stress and increased levels of cell death following Nelfinavir treatment. Research also identified a complex signalling pathway in which mTORC1 both regulates, and is regulated by the autophagy protein ULK1. Following observations of increased autophagy after treatment with Nelfinavir, a novel combinatorial therapeutic strategy was formulated that sought to exacerbate ER stress in conjunction with autophagy inhibition. Of clinical relevance, this novel strategy (using Food and Drug administration (FDA)-approved drugs) significantly and selectively induced cell death in TSC2-deficient cell lines and thus offers a promising avenue for future trials and research.

1. Introduction

The mechanistic target of rapamycin (mTOR), also known as the mammalian target of rapamycin, is critical in the normal function of a cell. mTOR regulates a large number of cellular processes that ultimately drive cell growth and proliferation. Although mTOR is best known for its regulation of protein synthesis, mTOR is also known to be involved in mitochondrial biogenesis/metabolism, lipid synthesis/metabolism, microtubule organisation as well as autophagy. mTOR is a highly evolutionary conserved serine/threonine protein kinase that belongs to the phosphoinositide 3-kinase related kinase (PIKK) family. mTOR forms two distinct multi-protein complexes: mTOR complex 1 (mTORC1) and mTOR complex 2 (mTORC2).

1.12 mTOR complex 1

mTORC1 consists of five known core components: mTOR, regulatory-associated protein of mTOR (Raptor), mammalian lethal with Sec13 protein 8 (mLST8 or GbL), proline-rich AKT substrate 40 kDa (PRAS40), and DEP-domain-containing mTOR-interacting protein (Deptor). mTORC1 is often considered as a master regulator of cellular growth, proliferation and metabolism. Some substrates of mTORC1 are well characterised. mTORC1 is able to phosphorylate eukaryotic initiation factor 4E-binding protein 1 (4E-BP1), a repressor of translation. Phosphorylation of 4E-BP1 by mTORC1 causes 4E-BP1 to detach from eukaryotic initiation factor 4E (eIF4E), which is bound to the 5'-end of mRNAs. 4E-BP1 dissociation from eIF4E promotes eIF4E-mediated translation of these mRNAs, which is often referred to as 5'-cap-dependent translation. Through 4E-BP1/eIF4E, mTORC1 drives protein synthesis and increases cellular growth. Some functions of mTORC1 can also occur indirectly via its downstream substrate, 70 kDa ribosomal protein S6 kinase 1 (S6K1), which is also considered as a regulator of cell growth (Fingar et al, 2002) and proliferation (Fingar et al, 2004). S6K1 is also a serine/threonine protein kinase and was originally named through phosphorylation of ribosomal protein S6 (rpS6). S6K1 can also phosphorylate eukaryotic elongation factor 2 kinase (eEF2K) involved in the elongation phase of protein translation regulate the levels of protein synthesis within

a cell. More recently, S6K1 was shown to phosphorylate a number of translation initiation factors including eIF3 and eIF4B to enhance efficiency of protein translation (Holz et al, 2005).

1.13 mTOR complex 2

mTORC2 is made up of six known core proteins, many of which are common to mTORC1: mTOR, rapamycin-insensitive companion of mTOR (Rictor), mLST8, protein observed with Rictor-1 (Protor-1), mammalian stress-activated protein kinase interacting protein (mSIN1) and Deptor. The main difference between the mTOR complexes, is that mTORC2 is not sensitive to inhibition with rapamycin (a potent inhibitor of mTORC1). Furthermore, mTORC2 also possesses Rictor instead of Raptor, where both these scaffold proteins are integral to either complex. Unlike mTORC1, the rapamycin insensitive mTORC2 is less well characterised. It is known that protein kinase B (PKB, also known as AKT) is activated by mTORC2 through phosphorylation at Ser473 (Hresko & Mueckler, 2005) and implicates mTORC2 in the regulation of a number of PKB-mediated cellular processes including survival, proliferation and metabolism. mTORC2 is also considered to be involved in cytoskeletal organisation as Rictor knockdown is known to affect actin polymerisation and alter cellular morphology involving Rho small G-proteins (Tee & Dunlop, 2009; Laplante & Sabatini, 2009).

1.14 Genetic disease and connections with mTOR

Given that mTORC1 and mTORC2 collectively regulate integral cellular processes such as protein synthesis, cellular growth, proliferation, survival as well as cytoskeletal reorganisation, it is unsurprising that genetic abnormalities in the genes upstream of these mTOR complexes give rise to an array of inherited genetic disorders. For instance, several syndromes are known to occur due to inherited mutations within tumour suppressor genes upstream of mTORC1, i.e., Tuberous Sclerosis Complex (TSC, caused by mutations within either *Tuberous Sclerosis Complex 1* or *2* (*TSC1/TSC2*)), Neurofibromatosis Type 1 (caused by mutations *NF1*), and Birt–Hogg–Dubé (BHD) syndrome (caused

by mutations in *Folliculin*). The pathology of these diseases is indicative of defects in cellular growth and proliferation with the development of benign tumours occurring in a variety of organs.

1.15 Tuberous Sclerosis Complex

TSC, a hamartoma syndrome that has a prevalence of around 1/5,000 to 1/10,000, occurs as a result of inactivating mutations in either of the tumour suppressors *TSC1* and *TSC2.* TSC1 and TSC2 function as a heterodimer upstream of mTORC1, and act as a GTPase activating protein (GAP) towards Rheb. By inactivating Rheb, through conversion of Rheb to a GDP-bound state, TSC1/TSC2 potently inhibits signal transduction through mTORC1. Inactivating mutations within either of these *TSC1* or *TSC2* genes leads to aberrant activation of mTORC1, which leads to increased cell growth and proliferation. As a result of this, TSC patients exhibit extensive tumour formation and growth in organs such as the kidneys and brain which can lead to severe clinical symptoms including seizures (see reviews Tee & Dunlop, 2009; Yang & Guan, 2007).

In addition to being prevalent in hamartoma syndromes, mutations in mTOR signalling pathway genes have also been found to be present in a number of sporadic cancers. Previous evidence indicates that loss of heterozygosity at a region spanning *TSC1* is observed in over 50% of bladder carcinomas and mutations in the gene occur at a frequency of 14.5%. It has also been identified that loss of heterozygosity of *TSC2* is also observed in a number of bladder carcinomas (Knowles et al, 2009).

1.16 mTORC1 and therapy in TSC

Considerable success has been achieved in developing therapies for patients with TSC. The drug rapamycin, an anti-fungal macrolide discovered on Easter Island (Rapa Nui), potently inhibits mTORC1 and cell growth. More recently, rapamycin has been used extensively in clinical trials as an anti-cancer agent. Rapamycin (as well as rapamycin analogues) have potent immunosuppressive and anti-proliferative properties and is clinically approved for use in patients. The mechanism by which

rapamycin acts to suppress mTORC1 is as a FKBP12/rapamycin (protein/drug) dimer. FKBP12 is considered an immunophil, although its involvement in the immune system is currently unknown. The FKBP12/rapamycin dimer associates with a FKBP12/rapamycin binding (FRB) domain within mTOR that lies distal from the kinase domain and blocks mTORC1 kinase activity. Presumably due to steric hindrance through differences in conformation. FKBP12/rapamycin does not inhibit the kinase activity of mTORC2.

Clinical trials have revealed that rapamycin is capable of significantly shrinking tumours in TSC patients. However, once treatment is ceased, the tumours regrow back to the original size or in some cases grow larger. This is perhaps unsurprising given that the rapamycin acts to restore the normal function of mTORC1. Rapamycin also promotes cell survival characteristics, which may in part be due to feedback mechanisms that activate mTORC2 and PKB as well as induce autophagy. An alternative therapeutic approach for TSC patients and those suffering from other conditions featuring aberrant mTORC1 activity could be to try to use a drug that selectively induces cell death as opposed to acting in a corrective manner. The idea of using combination therapy has also been suggested. Currently, using rapamycin in combination with autophagy inhibitors has shown additive effects in killing cell lines lacking *TSC2* (Yang & Guan, 2007; Sampson, 2009).

1.17 Endoplasmic Reticulum Stress

The Endoplasmic Reticulum (ER) is a cellular organelle that is responsible for ensuring that proteins are folded/processed correctly and that misfolded proteins are eliminated. Should the amount of unfolded or misfolded proteins within a cell increase, the ER becomes overloaded with unfolded protein to cause cellular stress. As a mechanism to offset this increased protein load on the ER, the ER activates a process termed the Unfolded Protein Response (UPR). During the UPR, the degradation of misfolded proteins and the ER's protein folding capacity is upregulated to remove the unfolded protein, whereas protein synthesis is down regulated to reduce further burden on the ER. This dual action of the UPR to remove unfolded protein and to prevent further accumulation of

proteins alleviates the stress and restores ER homeostasis. Initiators of the UPR are the type-I transmembrane kinases, inositol-requiring enzyme-1 (IRE-1) and PKR-like endoplasmic reticulum kinase (PERK), and a type-II transmembrane protein activating transcription factor-6 (ATF6). Activation of PERK causes the phosphorylation of eukaryotic translation initiation factor 2 alpha (eIF2a) which functions to globally reduce translation initiation. IRE-1 functions to activate c-Jun amino-terminal kinase (JNK) via tumour necrosis factor (TNF) receptor-associated factor-2 (TRAF-2) and apoptosis signal regulating kinase-1 (ASK-1). JNK then activates stress and inflammatory responses. IRE-1 also functions to cleave X-box binding protein-1 (XBP-1) mRNA which allows for the translation of the protein spliced form of XBP-1 (XBP-1S).

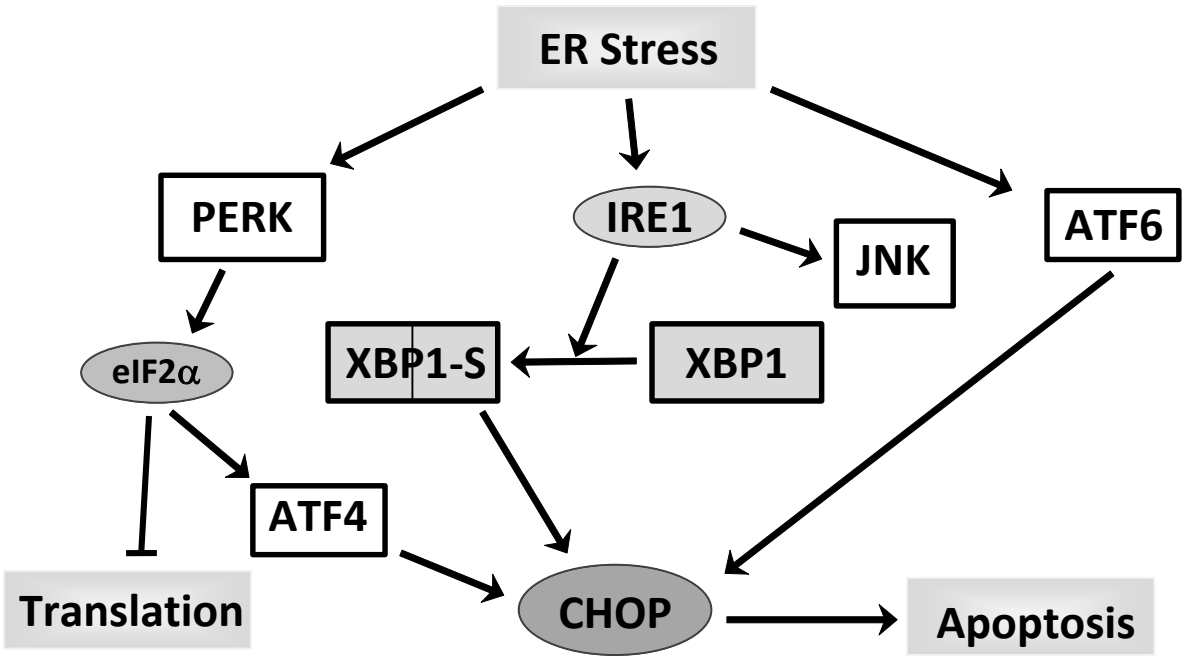

Figure 1.1: ER Stress Pathway. *eIF2α phosphorylation by PERK is a repressor of translation initiation, and if eIF2α is phosphorylated for a prolonged duration (which occurs when ER homeostasis is not efficiently restored), can lead to apoptosis through enhanced translation of ATF4 and gene-expression of CHOP. CHOP is further regulated through additional signalling pathways of the ER Stress pathway, through IRE1-mediated splicing of XBP1 and through transcriptional upregulation of ATF6.*

As a transcription factor, this spliced form functions as one of the main regulators of the ER. Autophagy, a cellular process responsible for the recycling of proteins within a cell and is also activated during the UPR to remove unfolded protein within the ER that further reduces ER stress. These multiple processes that coordinate to reduce ER stress clearly function in a pro-survival manner to attempt to allow the cell to recover. However, should ER stress occur at too high a level or for an extended duration, pro-apoptotic events are instead initiated as part of the ER stress response. The transcription factors XBP-1, ATF4 and ATF6 induce the expression of CCAAT/enhancer-binding protein homologous protein (CHOP). This protein regulates B-cell CLL/lymphoma 2 (Bcl-2) family members which function to induce apoptosis via the mitochondrial pathway. JNK signalling is also known to regulate the Bcl-2 proteins. In addition, IRE-1 and TRAF-2 recruit pro-caspase-12, an ER specific caspase (Hosoi et al, 2010; Ozcan et al, 2008; Healy et al, 2009). Please refer to figure 1.1 for a visual overview of the ER stress response pathway.

1.7 Autophagy

As mentioned previously, autophagy is a critical cell process that becomes activated during ER stress as a survival mechanism. Autophagy is employed by the cell to degrade and recycle proteins and organelles. During this process, organelles and protein aggregates become encapsulated in double membrane vesicles to form autophagosomes. Autophagosomes sequentially fuse with lysosomes and these vesicle structures are known as autolysosomes. The active fusion of autophagosomes to lysosomes is referred to as autophagic flux. This process requires vesicular trafficking and is a measure of autophagic activity. Once fusion has occurred, lysosomal hydrolases degrade sequestered material which allows for permeases to transport amino acids and lipids into the cytoplasm for use in either biosynthesis or the generation of energy (Nijholt et al, 2011; He & Klionsky, 2009).

1.8 mTORC1 and ULK1 in the regulation of autophagy

It is known that mTORC1 plays a significant role in the autophagic process and this occurs through negative regulation of Unc51 like kinase 1 (ULK1), the initiating Ser/Thr protein kinase for autophagy. In nutrient sufficient conditions, mTORC1 phosphorylates ULK1. mTORC1 phosphorylation of ULK1 restricts ULK1 kinase activity and represses autophagy. During nutrient deprivation or rapamycin treatment, the mTORC1-ULK1 complex dissociates and ULK1 kinase activity is no longer suppressed. ULK1 is then able to autophosphorylate as well as phosphorylate ATG13 and FIP200, which are tightly bound to ULK1 as a core complex. This activated ULK1-ATG13-FIP200 autophagy initiation complex localises to phagophores, the precursors of autophagosomes and is necessary for autophagy initiation. The nucleation process is then dependent on the production of Phosphatidylinositol 3-phosphate (PtdIns(3)P) by the protein complex comprised of class III phosphoinositide 3-kinase hVps34, Beclin 1 and p150/hVps35. The elongation and closure process results in the formation of double-membrane autophagosomes. This process is dependent on the activity of the large Atg16 protein complex which also facilitates lipidation and sequential localisation of MAP1LC3 (LC3) to the phagophore. As LC3 protein is synthesised, LC3 is cleaved to form the cytosolic LC3-I isoform. This then conjugates with phosphatidylethanolamine (PE) when autophagy becomes activated. This conjugated (or lipidated) isoform of LC3 is known as LC3-II and localises to the autophagosomal membrane where it is tethered. The final process of autophagosomal maturation is when the autophagosome fuses with a lysosome, which creates an autolysosome. It is here within the autolysosome that the encapsulated proteins and organelles become degraded by the acidic hydrolases that were contained within the lysosome (Rosenfeldt & Ryan, 2011).

At this time, AMBRA1 is the only known ULK1 substrate that is directly part of the autophagy machinery although it is not an integral component of the ULK1-Atg13-FIP200 complex (Di Bartolomeo et al, 2010). The identification of other downstream targets of ULK1 will be essential to better understand how ULK1 governs autophagy.

In addition to known interactions between mTORC1 and ULK1, it is known that AMPK positively regulates ULK1 through binding and phosphorylation. This interaction functions to induce autophagy during conditions of energy stress (Lee et al, 2010; Egan et al, 2011; Bach et al, 2011). It has also been reported that ULK1 can be further negatively regulated by AMPK, suggesting a possible feedback mechanism, where ULK1 phosphorylates all three AMPK subunits to reduce AMPK activation (Loffler et al, 2011; Kim et al, 2011).

1.9 Other forms of autophagy

In actuality, there are two other types of autophagy in addition to the above described process known as macroautophagy (Benbrook & Long, 2012). The second type of autophagy is known as chaperone-mediated autophagy which is controlled by heat shock protein A8 (HSPA8) (also known as heat shock cognate 70). During this process, the chaperone directly binds specific proteins which are then transported into the lysosome (Lee et al, 2011). The chaperone specifically targets molecules with a particular amino acid sequence, a motif related to KFERQ (Lys-Phe-Glu-Arg-Gln) (Dice et al, 1986). It may be that these sequences appear directly on the molecule's surface or alternatively, they may be in unexposed regions of the molecule and only become exposed as a result of damage or denaturation. Once HSPA8 has identified a molecule featuring this motif, it is transported to the lysosome where the chaperone docks to LAMP-2A (Lysosome-associated membrane protein type 2A). Here, numerous interactions with other chaperones occur to facilitate the transference of the molecule through LAMP-2A to another HSPA8 molecule within the lysosome where ultimately the molecule can be degraded (Agarraberes et al, 1997). Chaperone-mediated autophagy occurs after macroautophagy following nutrient deprivation in a mutually inhibitory fashion: as one form increases, the other decreases (Bejarano & Cuervo, 2010).

The third, less well described form of autophagy is known as microautophagy. In this process, aberrant molecules and organelles are engulfed directly into the lysosome where they are degraded and their components are then recycled (Lee et al, 2012). The first event of this process involves

active invagination at the lysosome membrane forming tube-like bodies (Müller et al, 2000). The subsequent processes of vesicle expansion, vesicle scission and vesicle degradation and recycling involve LC3 lipidation, mTOR controlled ubiquitin-like systems and other Atg machinery similar to macroautophagy (Li et al, 2012). Unlike the mutually inhibitory processes of macroautophagy and chaperone-mediated autophagy, microautophagy operates synergistically alongside them (Cuervo, 2004).

Unless expressly stated otherwise, when the term autophagy is used throughout this thesis, it is referring to the first form of autophagy, macroautophagy.

1.10 ER stress inducing agents and therapy

Given that cells lacking TSC2 exhibit constitutively activated mTORC1 signalling, higher levels of protein synthesis and disturbances in nutrient signalling, it is not surprising that TSC2 deficient cells show elevated levels of ER stress. Research has shown that TSC deficient cells have increased levels of PERK phosphorylation, CHOP and XBP-1s, showing that they are exhibiting higher basal levels of ER stress and have activated the UPR. It was also shown that this stress response could be ceased upon reconstitution of TSC2 in deficient cells (Ozcan et al, 2008).

There might be potential therapy options to treat human diseases (such as cancer) featuring heightened mTORC1 activation, by further intensifying the already present ER stress. For instance, cancerous cells with heightened mTORC1 activation would already be experiencing an increased level of ER stress compared to normal cells. By using an agent that would further enhance ER stress, it might be possible that these cancerous cells with aberrant mTORC1 signalling would be more susceptible to trigger the pro-apoptotic mechanism of the UPR, as the level and duration of ER stress would be pushed significantly greater. While in contrast, the moderately stressed normal cells would only experience the pro-survival aspects of the UPR and fully compensate.

1.11 *Nelfinavir as an ER stress inducer*

Nelfinavir is a clinically approved anti-retroviral drug that has been used for over a decade to treat patients suffering from HIV infection. Following the observation that Nelfinavir caused regression of Kaposi's sarcomas in HIV patients, this drug has been shown to induce apoptosis in a number of different tumour cell lines. Although the exact mechanisms of Nelfinavir's anti-tumour effect have not been elucidated, it has been observed that Nelfinavir is capable of inducing ER stress and autophagy. This effect appears to occur due to the drugs ability to inhibit proteases within a cell's proteasome. As a result, misfolded and unfolded proteins would accumulate within the cell, ER stress would occur and the UPR would become activated. Because of these drug effects in patients as well as limited toxicity, it was postulated that Nelfinavir might be a potential agent to treat diseases with aberrant mTORC1 activity, which already have a high level of basal ER stress (Cho et al, 2009).

2. Methods and Materials

2.1 Plasmid details

HA-Raptor (Addgene Inc, Massachuttes, U.S.A.),

V5 tagged ULK1 and ULK2 (generated by Dr. Elaine A. Dunlop (Cardiff University) using gateway system (Invitrogen, Paisely, UK),

pRK7, S6K1 and HA-S6K1 (Kind gift from Prof. John Blenis (Harvard University),

Q64LRheb generated via site-directed mutagenesis of the Flag-Rheb/pRK7 vector that was generated by Dr A.R.Tee (Cardiff University).

Poly Ubiquitinated protein Plasmid (Addgene),

shRNA constructs including ULK1, ULK2 and non-target control (MISSION shRNA SIGMA).

2.2 Antibodies and other biochemicals

Cell Signaling Technology, Inc., Massachuttes, U.S.A:

Anti eIF2α, #9722

Anti Phospho-eIF2α (Ser51), #3597

Anti rpS6, #2217

Anti Phospho-rpS6 (Ser235/236), #4858

Anti S6K1, #2708

Anti Phospho-S6K1 (Thr389), #9234

Anti AMPK, #2603

Anti Phospho-AMPK (Thr172), #2535

Anti ACC, #3676

Anti Phospho-ACC (Ser79), #3676

Anti Beta Actin, #8457

Anti AKT, #4685

Anti Phospho AKT (Thr308). #4056; Anti Phospho AKT (Ser473). #4060

Santa Cruz, California, U.S.A.:

Anti ULK1 (N-17), #sc-10900

Anti ULK2 (E-19), #sc-10907

Anti Rheb (N-19). #sc-6342

Other:

Anti HA Mouse (16B12) #ab24779 (Abcam plc, Cambridge, UK),

Anti HA Rat (clone 3F10) #11867423001 (Roche, Basel, Switzerland),

Anti V5 (2F11F7) #377500 (Invitrogen),

Anti LC3 #NB100-2220 (Novus Biologicals),

Anti p62 (SQSTM1) C-terminal antibody (GP62-C) #DS-160211 (Progen Biotechnik)

Anti Ubiquitin #BML-PW8810-0100 (Bio Mol),

Secondary Antibodies (SIGMA).

2.3 Cell Lines

CRUK 293 cells, HEK 293 cells (from ATCC), $TSC1^{-/-}$ and $TSC2^{-/-}$ $p53^{-/-}$ mouse embryonic fibroblasts (MEFs), ELT3-V3 and ELT3-T3 were utilised in experiments.

2.4 Drugs

Sigma-Aldrich Company Ltd., Dorset, UK:

Nelfinavir (Viracept tablets) - dissolved in 100% Ethanol,

Thapsigargin, Celecoxib, MG132, Bafilomycin A1 - dissolved in DMSO,

Chloroquine - dissolved in double distilled deionised water,

Insulin in solution.

Calbiochem Ltd:

Rapamycin - dissolved in DMSO.

2.5 Cell culture and transfection

CRUK293 and HEK293 cells were maintained in Dulbecco's Modified Eagle's Medium (DMEM) also containing 10% foetal calf serum (FCS), 100 μg/ml penicillin and 100 μg/ml streptomycin (Gibco, Paisley, UK). Cells were stored in cryogenic vials under liquid nitrogen in freeze media (8 % DMSO in FCS). Cells were washed with 1ml Optimem (Gibco), 1.8 mls DMEM containing 10% FCS was added and Lipofectamine 2000 (Invitrogen) transfections were performed to introduce Q64L Rheb or pRk7 empty vector to the CRUK293 cells or combinations of V5 tagged ULK1, V5 tagged ULK2, HA tagged Raptor, Rheb, S6K1 and pRK7 to the HEK293 cells. At 4 h post-transfection, the media on the cells was replaced with 2 mls DMEM containing 10% FCS, 100 μg/ml penicillin and 100 μg/ml streptomycin. Cells were then incubated at 37 ^{o}C and harvested 24h later.

2.6 Drug treatments, Cell lysis and Cell buffers

Drugs were dissolved in a suitable solvent as indicated above. For cell treatments, suitable dilutions were made of the drug master stocks and DMEM so as to produce the final drug concentrations required (as indicated, along with treatment times, in the figure legends of the results section).

Cells were lysed in Blenis Lysis Buffer (unless stated otherwise), 200μl per 35mm plate:

10 mM KPO_4 / 1mM EDTA pH 7.05

5 mM EGTA pH 7.2

10 mM $MgCl_2$

50 mM β-Glycerol Phosphate pH 7.2

0.5% NP-40, 0.1% (v/v)Brij-35

1 mM $Na_2VO_4^{3-}$

2 mM DTT

40 µg/ml PMSF

50 µg/ml Pepstatin A

10 µg/ml Leupeptin

2.7 Western blotting

Protein levels of samples were standardised by performing a Bradford assay. Samples from figures 1 and 3 were boiled at 95 °C for 5 min and resolved on a 12% Protogel (National Diagnostics, Atlanta, U.S.A.) whereas other samples were boiled at 70°C for 10 min and resolved on 3-8 % or 4-12 % Novex precast gradient gels (Invitrogen) (200V for 90 mins). Proteins were transferred to Polyvinylidene Difluoride (PVDF) membranes (Millipore) (25V for 2 hours) , blocked in 5 % (w/v) dry milk powder/Tris buffered saline 0.1 % (v/v) Tween (TBS-T), then probed using the required primary antibody and Horse Radish Peroxidase (HRP)-conjugated secondary antibody (Sigma-Aldrich). Proteins were visualised using Enhanced Chemiluminescent (ECL) solution (GE Healthcare) and Fujifilm Super RX X-ray film (Jencoms (a VWR Division), Leicestershire, UK).

2.8 S6K1 assay

HEK293 cells were transfected with combinations of HA-S6K1, V5-ULK1, Rheb and pRK7 using Lipofectamine 2000 (Life Technology Ltd.) according to the manufacturer's protocol. 4 h post-transfection, media was changed on the cells and they were incubated for 24 h before lysis. Cells were lysed using 10 mM K2PO4 (pH 7.4), 1 mM EDTA pH 7.05, 5 mM EGTA pH 7.2, 10 mM MgCl2, 50 mM β-Glycerol Phosphate, 1 mM Na3VO4, 2 mM DTT, 0.5 % (v/v) NP-40, 0.1 % (v/v) Brij-35 and protease inhibitors. Lysates were incubated for 2 h at 4^{o}C with protein G-Sepharose beads, and anti-HA antibody. HA immunoprecipitates were washed once each with Buffer A (10 mM Tris, 1 % (v/v) nonidet P-40, 0.5 % (v/v) sodium deoxycholate, 100 mM NaCl, 1 mM EDTA and protease inhibitors, pH 7.2), Buffer B (10 mM Tris, 0.1 % (v/v) Nonidet P-40, 0.5 % (v/v) sodium deoxycholate, 1 M NaCl,

1 mM EDTA, plus protease inhibitors pH 7.2), and ST Buffer (50 mM Tris-HCL, 5 mM Tris-base, 150 mM NaCl, plus protease inhibitors, pH 7.2). S6K1 complexed beads were incubated for 10 min at 30^{o}C in 20 mM HEPES, 10 mM MgCl2, 50 µM ATP unlabelled, 5 µCi of [γ-^{32}P]ATP (PerkinElmer Life Sciences), 3 ng/µl PKI, pH 7.2, in the presence of recombinant GST-S6 peptide (32 final amino acids of ribosomal S6). Reactions were subjected to SDS-PAGE, and the relative levels of [^{32}P]-labelled GST-S6 was determined by autoradiography. Setting up of the experiments was carried out by me, while handling of the radioactive material was performed by Dr A. Tee.

2.9 ULK1 kinase assay

HEK293 cells were washed and incubated in 2 ml of phosphate-free DMEM containing 0.2 mCi [32P]-orthophosphate for 4 h. Following incubation, cells were treated with rapamyicn and insulin stimulated as required. After these treatments, the cells were lysed in mTORC1 lysis buffer (40 mM HEPES (pH 7.4), 2 mM EDTA, 10 mM β-glycerophosphate, 400 mM NaCl, 0.3% (w/v) CHAPS and protease inhibitors) and subsequently sonicated. ULK1 was immunoprecipitated for 2 h with anti-ULK1 antibody (N-terminal from Santa Cruz) bound to protein G-Sepharose. The sepharose beads were washed 3 times with the mTORC1 lysis buffer. Immunopreciptated radiolabelled [32P]-ULK1 was resolved on SDS-PAGE, fixed in 40% (v/v) methanol, 10% (v/v) acetic acid, dried down in a gel dryer and then exposed to film.

2.10 RNA Extraction

RNA was extracted from 35 mm^2 tissue culture plates using RNeasy Plus Mini Kit (Qiagen) using the suppliers protocol.

2.11 Reverse Transcription (RT) Polymerase Chain Reaction (PCR)

1 µg of RNA was reverse transcribed using Quantitect Reverse Transcription Kit (Qiagen) using the protocol of the supplier.

2.12 Quantitative real time PCR (QPCR)

QPCR reactions were set up using Sybr Green PCR Master mix (Qiagen), cDNA and distilled H_2O following the suppliers protocol. The 12.5 µl reactions were placed into 96 well plates and were run using the following protocol:

Initial Denaturation - 95°C for 15 mins – 1 Cycle

Denaturation - 94°C for 15 secs

Annealing - 55°C for 30 secs – 40 Cycles

Extension - 72°C for 40 secs

2.13 Cyquant Assay

CyQUANT® Cell Proliferation Assays | Life Technologies - Invitrogen

Experiments were undertaken according to manufacturer's instructions. The CyQUANT reagents were prepared in advance by combining 550 µl CyQUANT GR dye with 11 mls Cell lysis buffer. Concentrated cell suspensions in growth medium were generated and then serial dilutions were prepared and transferred to a clear based 96 well plate. A hemacytometer was used to calculate the dilutions necessary to give 2000 cells per 200 µl in each well. The plates were incubated overnight at 37°C to allow the cells to adhere. Each well was then drug treated and incubated for a further 24 hours. Following incubation, the plates were gently inverted and blotted on paper towels to remove

the medium. 200 µl of CyQUANT reagent was added to each well and the plates were incubated at room temperature for 5 mins, wrapped in aluminium foil to protect from light. Fluorescence was then measured in a microplate reader with filters for ~480 nm excitation and ~520 nm emission maxima. To quantify cell number, a dilution series was set up from a concentrated cell suspension in which cell number had been calculated using a hemacytometer. The assay was performed on these dilutions to produce a standard curve in which cell number could be determined from the fluorescence values.

2.14 Cell Death Assay

Cell Death Detection ELISA - Roche Applied Science.

Experiments were undertaken according to manufacturer's instructions. The immunoreagent was prepared in advance by mixing 1/20 volume Anti-DNA-POD, 1/20 volume Anti-histone-biotin with 18/20 volumes Incubation buffer. Cells were grown and drug treated in a 96 well plate as described previously for the CyQUANT assay. Following the drug treatments, the plate was centrifuged for 10 mins at 200 x g and the supernatant was carefully removed from the wells using a pipette. The cell pellets were then resuspended in 200 µl lysis buffer and incubated at room temperature for 30 mins. Following incubation, the lysates were centrifuged at 200 x g for 10 mins before 20 µl of supernatant was transferred into the streptavidin coated multiwell plate. 80 µl of immunoreagent was added to each well and an adhesive cover foil was added to the plate which was then incubated on a shaker at 300 rpm for 2 hours at room temperature. The solution was then removed from each well using a pipette and each well was rinsed 3 times with 300 µl incubation buffer (which was carefully removed following the final rinse). 100 µl ABTS solution was added to each well and the plate was incubated on a shaker at 250 rpm for 10 mins at room temperature. Finally, 100 µl ABTS Stop solution was added to each well. A plate reader was used to measure absorbance at 405 nm.

2.15 Replicates and data analysis

All experiments were performed at least in triplicate. For numerical data, Microsoft Excel was used to calculate standard error bars and these are displayed on the graphs. Statistical significance was confirmed by performing a Student's t-test and p-values less than 0.05 are indicated on graphs by *. For other experiments (including western blots), the results shown are representative of the observations seen in three or more separate experiments.

3. Results

3.1 Nelfinavir induces ER stress

Previous preliminary research by Dr Davies within Cancer and Genetics (Cardiff University) upon screening various clinically approved drugs implied Nelfinavir might induce selective toxicity to mouse embryonic fibroblasts (MEFs) that lack TSC2. Although Nelfinavir is commonly used as an anti-HIV drug, it is also being tested as an anti-cancer agent. One drug action of Nelfinavir is through enhancing ER stress. Given that Nelfinavir is an ER stress inducer (Cho et al, 2009), the sensitivity of these *TSC2* null cells to Nelfinavir might be as a consequence of an already existing ER stress burden.

The first aim of this work was to determine the levels of ER stress within cell models of heightened mTORC1 signalling upon treatment of Nelfinavir. To examine whether Nelfinavir was capable of elevating levels of ER stress within cells, eIF2α phosphorylation at Ser51 was examined in HEK293 cells (Figure 3.1). Phosphorylation of eIF2α at Ser51 is one of the most commonly utilised indicators of ER stress elevation that occurs in the early stages of the ER stress response (Saito et al, 2011). Upon treatment with Nelfinavir, western blots indicate a modest elevation of eIF2α phosphorylation in insulin-stimulated HEK293 cells relative to the untreated controls (Figure 3.1).

Such a finding implies that you need to drive cell growth, i.e., through activation of the PI3K/Akt pathway, in combination of Nelfinavir treatment to see a stress response via eIF2α phosphorylation. The effects of Nelfinavir on immediate ER stress markers, autophagy and mTORC1 signalling (which are part of the ER stress response) was then examined. Protein levels of p62 were analysed to examine whether autophagy might be affected in cells treated with Nelfinavir. The marked reduction in p62 upon Nelfinavir treatment, indicates induction of autophagy, as was previously described with use of Nelfinavir on cell lines as well as in animal models (Gills et al, 2007). Celecoxib was then compared alongside Nelfinavir. This drug is a COX-2 (cyclooxygenase-2) inhibitor that has also been suggested to exacerbate ER stress (Huang et al, 2013). The results indicate that this drug also modestly enhanced the level of eIF2α phosphorylation under insulin stimulation. Of interest,

Nelfinavir treatment potently reduced rS6 phosphorylation upon insulin stimulation, while Celecoxib had little effect. Unlike Nelfinavir, Celecoxib had no effect on the protein levels of p62, which shows that Nelfinavir induces autophagy through mechanisms that are separate from ER stress induction (given that both Nelfinavir and Celecoxib are both ER stress inducers).

Figure 3.1

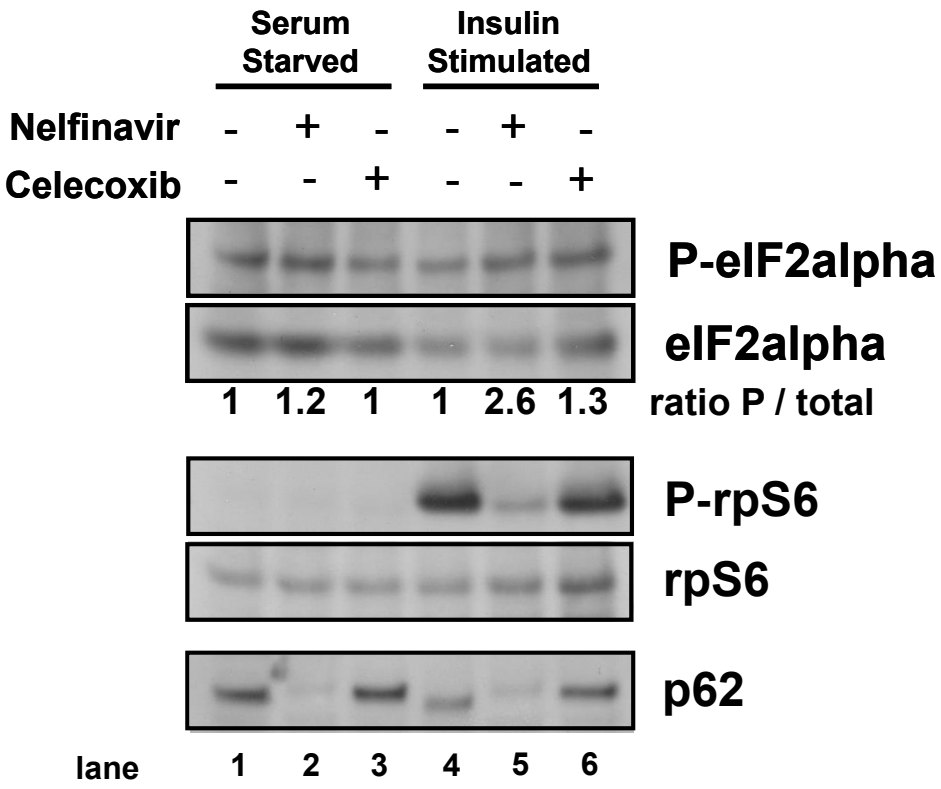

Figure 3.1. Nelfinavir increases eIF2α phosphorylation. *HEK293 cells (serum starved/insulin stimulated) were treated with Nelfinavir (30 μM) or Celecoxib (50 μM) for 24 h and total lysates were examined by western blotting. Modest increases in eIF2α phosphorylation were observed in the Nelfinavir conditions in addition to significant reductions in the levels of p62 and rpS6 phosphorylation. These observations are indicative of potent induction of autophagy by Nelfinavir and subsequent repression of mTOR signalling. Densitometry was carried out using Image J (1.47v).*

3.2 ER stress is greater in cells with constitutively activated mTOR signalling

The idea that constitutively active mTORC1 might enhance basal levels of ER stress was then tested. This was done using a GTP-bound mutant of Rheb (Q64L), which has lost its intrinsic GTPase activity. Consequently, RhebQ64L is a potent activator of mTORC1 when expressed in HEK293 cells (figure 3.2), as observed by an increase in rpS6 phosphorylation when RhebQ64L was expressed.

Figure 3.2

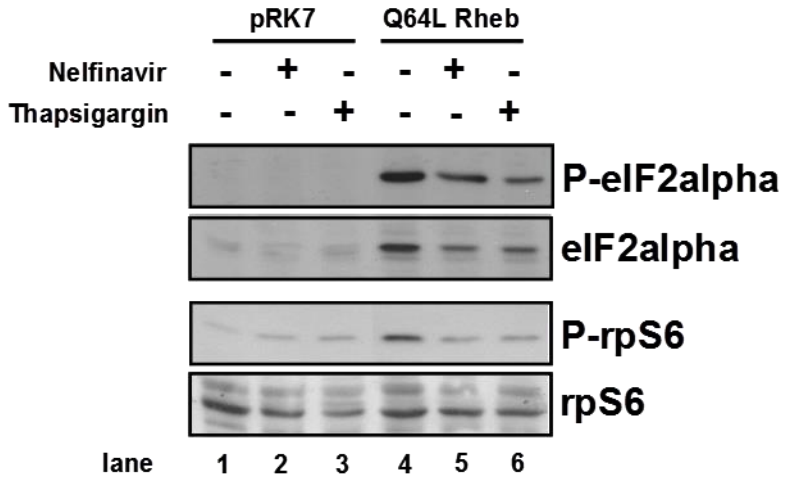

Figure 3.2. Increased levels of eIF2α phosphorylation are observed in cells with constitutively activated mTOR signalling compared to wild type cells. *This suggests increased basal levels of ER stress in cells with aberrant mTORC1 activity. CRUK 293 cells were transfected as described in 'materials and methods' with either 2 µg empty pRK7 or 2 µg Q64L Rheb. Cells were then treated with either 20 µM Nelfinavir or 300 nM Thapsigargin for 24 h. Cells were then lysed in Blenis Lysis Buffer and protein levels were assessed via Western blotting.*

Importantly, when Rheb/mTORC1 signalling was enhanced, the levels of eIF2α phosphorylation was substantially elevated. Such data supports the idea that constitutive activation of mTORC1 can lead to high levels of ER stress. Treatment of either Nelfinavir or Tharpsigargin for 30 min, was

sufficient to block this high level of eIF2α phosphorylation, which is likely due to inhibition of mTORC1 (as observed by a reduction in rpS6 phosphorylation). Both Nelfinavir and Thapsigargin are inducers of autophagy and autophagy is known to repress mTORC1 signalling (via an undetermined mechanism). Therefore, it is possible that autophagy induction by both Nelfinavir and Thapsigargin could lead to inhibition of mTORC1.

3.3 TSC deficient cells have a truncated ER stress response

Having made these observations relating to Nelfinavir's effects on eIF2α phosphorylation, the effects on another marker of ER stress, CHOP, were then examined. To achieve this, QPCR was employed to measure mRNA levels in *TSC2-/-* and *TSC2+/+* MEFS following treatments with varying concentrations of Nelfinavir (Figure 3.3). Of interest, lower levels of CHOP mRNA were observed in the *TSC2-/-* MEFs following treatment (when compared to the controls). This suggests that cells with aberrant mTORC1 activity have a truncated ER stress response. It should be noted that mRNA levels do not necessarily mirror the levels of protein and thus future experiments should be performed to confirm CHOP protein levels and confirm this observation.

One of the key elements of the ER stress response pathway is autophagy, where autophagy heavily influences whether a cell survives or undergoes apoptosis following ER stress. Given the observation that Nelfinavir seemed to potently activate autophagy, the next stage of research sought to gain a better understanding of the molecular mechanisms of autophagy and how mTORC1 is involved in this ER stress response pathway. This line of investigation also sought to determine the apparent resistance of TSC2-deficient cells to ER stress induced by Nelfinavir.

Figure 3.3

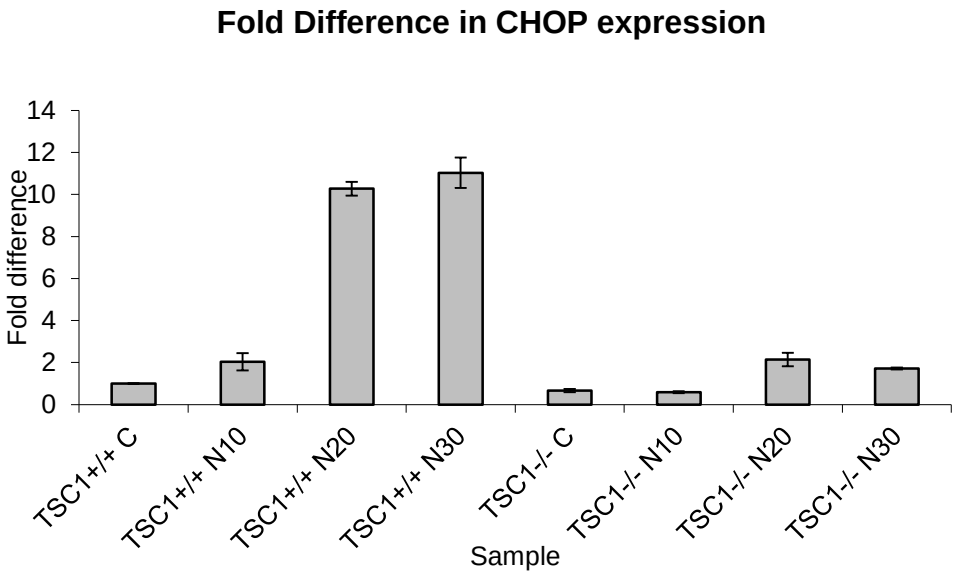

Figure 3.3. Nelfivavir does not induce higher levels of CHOP expressions in TSC1 deficient cells. *Following 24 h incubation in the presence of 10 µM, 20 µM or 30 µM Nelfinavir, RNA was extracted from $TSC1^{+/+}$ and $TSC1^{-/-}$ cells (following manufacturer's instructions in the QIAGEN kit) and subjected to QPCR analysis using primers specific to CHOP. Results were standardised to a β-actin control and the fold difference of CHOP expression relative to the $TSC1^{+/+}$ control was calculated. Levels of CHOP mRNA were lower in all $TSC1^{-/-}$ cell conditions inferring that ER stress is lower. As suggested by other research, a lower level of CHOP mRNA may be due to the ER stress response being truncated in the $TSC1^{-/-}$ cells (Kang et al, 2011).*

3.4 ULK1 phosphorylates Raptor

To examine autophagy in more detail with regards to mTORC1, an ULK1 mammalian expression vector was used. ULK1 is one of the principal components of the autophagy pathway in eukaryotes. Firstly, the impact of ULK1 activity on mTORC1 signalling was assessed by co-transfecting ULK1 and Raptor into HEK293 cells. In these experiments, an upwards mobility shift was observed when Raptor was resolved in SDS-PAGE. This is indicative of a phosphorylation event, which was not

observed in the control conditions in which ULK1 was not co-transfected (Figure 3.4). Interestingly, a Raptor mobility shift (albeit to a lesser extent) was also observed when ULK2 was co-transfected in place of ULK1, suggesting that there is some functional redundancy between these proteins. When Raptor protein that was excised from gels was subjected to MALDI-TOF (thanks to Prof. John Blenis (Harvard University, Boston, USA)), multiple ULK1-mediated protein phosphorylation events were identified within Raptor (please refer to discussion for more information and (Dunlop et al, 2011)).

Figure 3.4

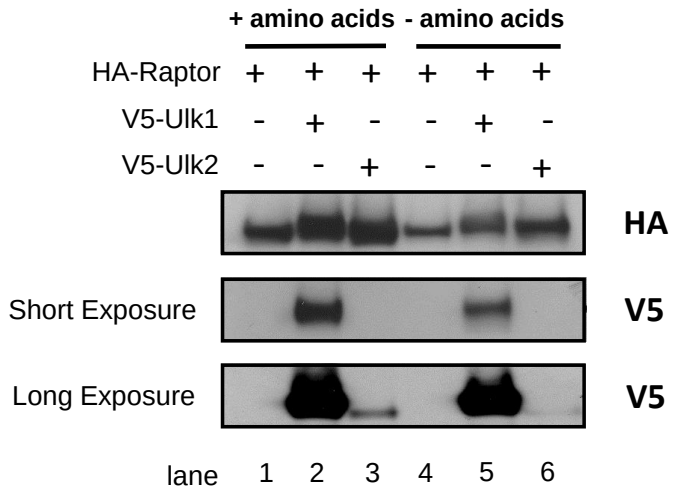

Figure 3.4. ULK1 causes a mobility shift of Raptor, indicative of a phosphorylation event(s). *HEK 293 cells were transfected with 1 µg HA-Raptor and either 1 µg V5-ULK1 with 3 µg pCDNA3 or 4 µg ULK2. Following incubation overnight, cells were either amino acid starved in Kreb's Ringer Buffer (made up of 115 nm NaCl, 5 mM KCl, 10 mM $NaHCO_3$, 2.5 mM $MgCl_2$, 2.5 mM $CaCl_2$, 20 mM HEPES and dH_2O with a pH of 7.4) or DMEM plus FCS was added. After 4 h, cells were lysed and the proteins were visualised through Western blotting. The mobility shift observed is likely due to the phosphorylation of Raptor by ULK1. The finding that the mobility shift also occurs due to ULK2 indicated that some level of functional redundancy exists between ULK1 and ULK2.*

3.5 ULK1 inhibits mTORC1

It was also observed that over-expression of ULK1 was capable of potently reducing the levels of S6K1 phosphorylation at Thr389 and also to reduce the levels of S6K1 kinase activity against recombinant ribosomal protein S6 (rpS6) (figure 3.5). This data implies that ULK1-mediated phosphorylation of Raptor is inhibitory to signal transduction through mTORC1.

Figure 3.5

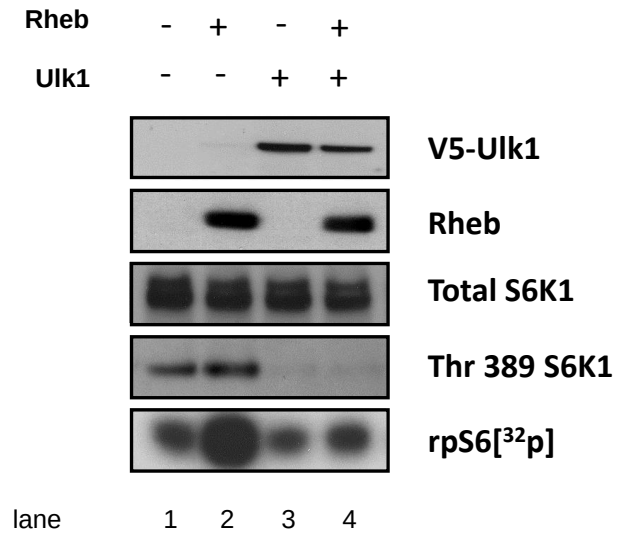

Figure 3.5. ULK1 inhibits mTOR activity. *HEK 293 cells were transfected and immunoprecipitations performed as described in the S6K1 Assay section of 'material and methods'. Total lysates were used to assess levels of V5-ULK1, Rheb and Thr389 S6K1. Results indicate a large reduction in Thr389 phosphorylation of S6K1 and in the levels of rpS6[^{32}p]. This is indicative of a substantial inhibition of the mTORC1 pathway.*

3.6 ULK1 knockdown alleviates mTORC1 inhibition

These initial observations that ULK1 might be involved as a negative regulator of mTORC1 were reinforced by undertaking ULK1 knockdown experiments (figure 3.6). Upon transfecting shRNA to target ULK1 mRNA, mTORC1 signalling in HEK293 cells was observed to be elevated (as indicated by enhanced phosphorylation of rpS6).

Figure 3.6

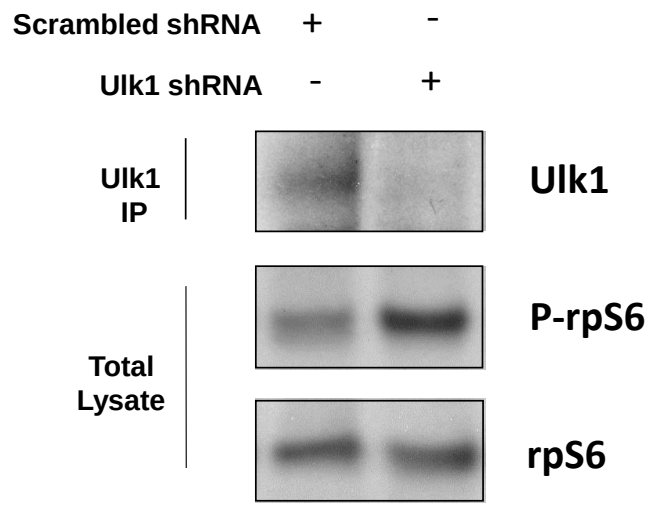

Figure 3.6. Inhibition of mTORC1 is alleviated following knockdown of ULK1. *HEK 293 cells were transfected with either scrambled shRNA (non-target) or ULK1 shRNA vectors, where indicated. Immunoprecipitations were undertaken to assess levels of ULK1 (and thus confirm successful knockdown) and total lysates were used to examine rpS6 phosphorylation. As shown by increased rpS6 phosphorylation, knockdown of ULK1 increases/restores mTORC1 activity.*

3.7 mTORC1 inhibition by ULK1 occurs independently of AMPK signalling

It was speculated that AMP-dependent protein kinase (AMPK) signalling may also be involved in mTORC1 repression by ULK1, given that AMPK and ULK1 are known to interact and AMPK

can enhance ULK1 activation. Furthermore, AMPK is known to phosphorylate Raptor directly (Gwinn et al. 2008). Phosphorylation levels of AMPK and ACC (acetyl-CoA carboxylase, a downstream substrate of AMPK) were therefore analysed following different co-transfections with ULK1, ULK2 and Raptor. No appreciable differences were observed in the levels of AMPK and ACC phosphorylation suggesting that the Raptor mobility shift and mTORC1 inhibition is occurring independently of AMPK signalling (figure 3.7).

Figure 3.7

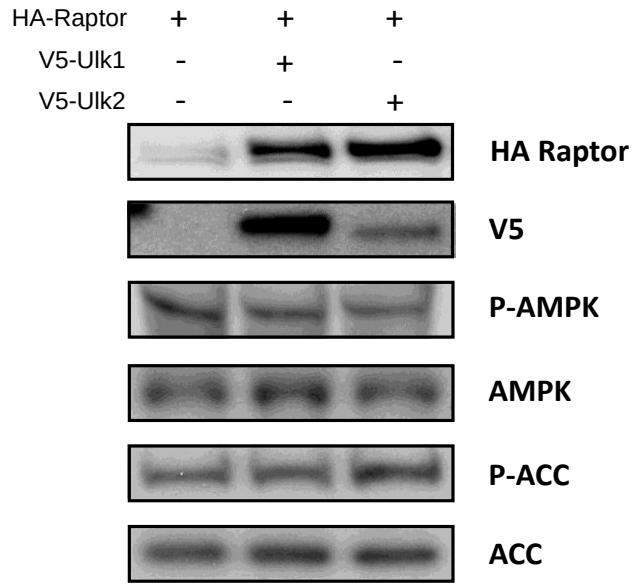

Figure 3.7. Inhibition of mTOR by ULK1 occurs independently of AMPK signalling. *HEK 293 cells were transfected as described previously with HA-Raptor and V5-ULK1 or V5-ULK2. Western blotting of total lysates was used to assess phosphorylation levels of AMPK and ACC. As increases in AMPK and ACC phosphorylation were not observed alongside the Raptor mobility shift, the inhibition of mTORC1 by ULK1 and ULK2 is assumed to be independent of AMPK signalling.*

3.8 mTORC1 signalling inhibits ULK1

Following these observations of the effects of ULK1 to repress mTORC1 signalling, the effects of mTORC1 on ULK1 were then examined. Autophosphorylation of ULK1 (which is considered a measure of ULK1 kinase activity) was significantly reduced upon 30 min insulin stimulation and was partially rescued upon rapamycin treatment, suggesting that mTORC1 was repressing ULK1 (figure 3.8). To examine mTORC1 signalling in more detail, Rheb was overexpressed in HEK293 cells and the total protein levels of ULK1 was measured. Interestingly, lower levels of ULK1 protein were observed in the conditions of Rheb over-expression suggesting that some of the reduction/inhibition of ULK1 activity is likely due to mTORC1-mediated degradation of ULK1 (figure 3.9).

Figure 3.8

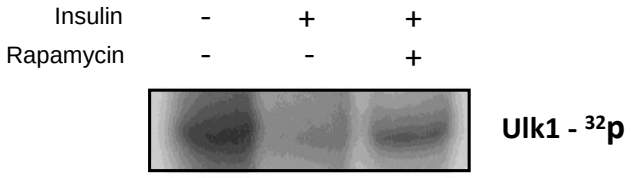

Figure 3.8. mTORC1 signalling inhibits ULK1 through ULK1 degradation. *[^{32}P]-orthophosphate in vivo radiolabelling of HEK 293 cells were carried out to examine [^{32}P]-incorporation into ULK1 after being immunoprecipitated. Cells were starved and then stimulated with insulin for 30 min in the presence or absence of 100 nM Rapamycin (30 min pre-treatment). Levels of ULK1[^{32}p] were significantly reduced following insulin stimulation but this effect was minimised in the presence of Rapamycin. This evidence indicates that mTORC1 signalling is inhibitory towards ULK1 and therefore autophagy.*

Given these observations, it seems reasonable to conclude that a complex inhibitory interplay exists between mTORC1 and the ULK1 signalling pathways (for a potential mechanism see figure

3.10). Having completed this functional work, the next stage of research was to return to investigating the therapeutic potential of Nelfinavir with regards to also targeting autophagy.

Figure 3.9

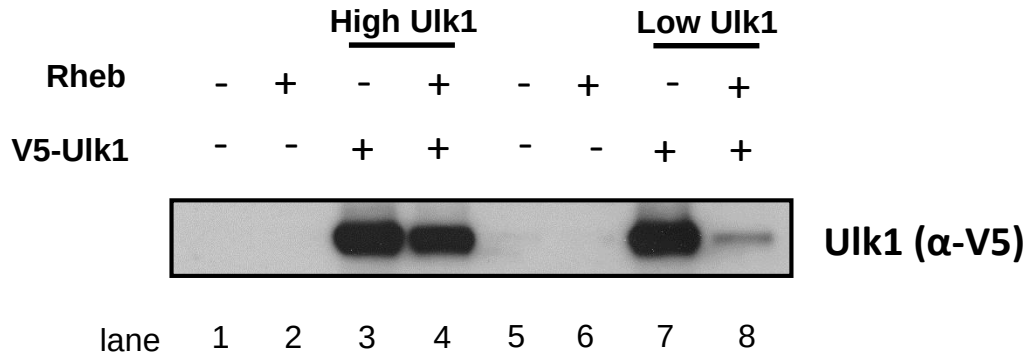

Figure 3.9. Rheb expressing HEK 293 cells have reduced stability of ULK1 protein. *HEK 293 cells were transfected with V5-ULK1 and Rheb as described previously (high ULK1 was 4 µg plasmid versus low ULK1 that was 1 µg plasmid). Relative levels of V5-ULK1 protein was determined from 25 µg of total protein cell lysates. In the presence of Rheb expression, which is known to potently enhance mTORC1 signalling, significantly lower levels of ULK1 protein was observed. Such evidence suggests that increased mTORC1 activity may cause increase degradation of ULK1.*

Figure 3.10

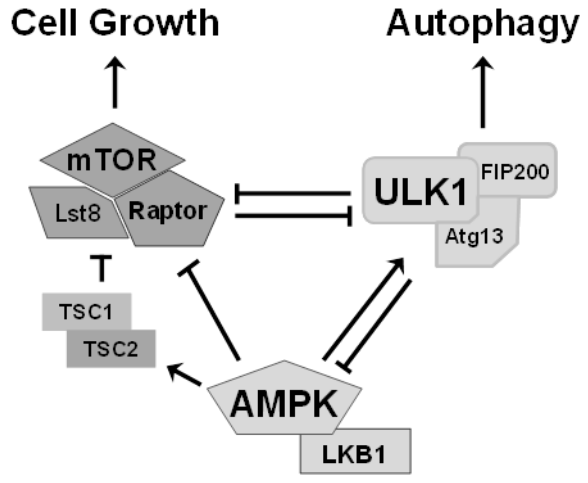

Figure 3.10. Illustrative diagram of mTOR and ULK1 interactions. *An inhibitory feedback network appears to exist between the autophagy and mTOR pathways. Additional regulation occurs through AMPK signalling which functions to inhibit mTOR and activate autophagy.*

3.9 Nelfinavir induces autophagy and inhibits mTORC1

It was shown in previous experiments that Nelfinavir, similarly to the positive control of Thapsigargin, was capable of increasing phosphorylation of eIF2α and thus increase the levels of ER stress. It was also observed that Nelfinavir treatment significantly reduced levels of rpS6 phosphorylation suggesting that Nelfinavir was potently inhibiting signal transduction through mTORC1. Given that experiments had previously established that ULK1/autophagy were inhibitory towards mTORC1, it was reasonable to assume that the reduction in mTORC1 activity upon Nelfinavir treatment was due (in part) to an induction of autophagy. This hypothesis was supported by reductions in the level of p62 and increases in the proportion of the lower lipidated form of LC3 (LC3-II) in cells treated with Nelfinavir, which are both indicators of increased autophagy. Protein levels of ULK1 were also shown to be elevated upon treatment with Nelfinavir (figure 3.11). As expected, potent impairment of rpS6 phosphorylation was also observed upon treatment with Nelfinavir, as one would expect given the increased levels of ULK1 protein and enhanced autophagy.

These findings suggest that autophagy is being exploited by cells as a survival mechanism to withstand the stress induced by Nelfinavir (presumably through ER stress) as well as Thapsigargin. It was postulated that Nelfinavir could induce ER stress through inhibition of the proteosome (Kraus et al, 2013).

Figure 3.11

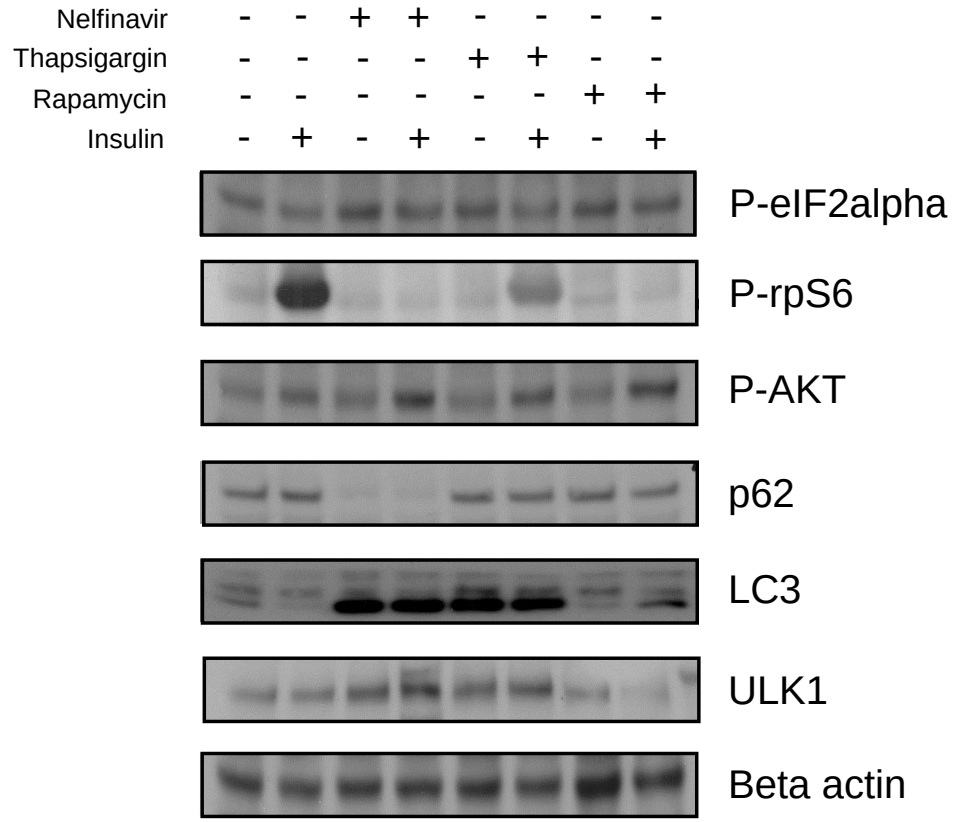

Figure 3.11. Nelfinavir causes induction of autophagy and inhibition of mTORC1. *HEK 293 cells were treated as described previously with Nelfinavir (30 µM). The positive control of Thapsigargin (300 nM) was also included as well as a Rapamycin (100 nm) control. Reductions in p62 and rpS6 phosphorylation and increases in the lower isoform of lipidated LC3 (LC3-II) indicates upregulation of autophagy and inhibiton of mTORC1 in both the Nelfinavir and Thapsigargin conditions. Also in these conditions, increased levels of ULK1 protein was observed, which again highlights increased protein stability of ULK1 when mTORC1 signalling is reduced.*

3.10 Nelfinavir does not significantly inhibit the proteasome

To examine whether Nelfinavir could inhibit the proteosome within HEK293 cells, removal of polyubiquitinated protein was assessed after Nelfinavir treatment. HA-tagged Ubiquitin protein was

expressed in these HEK293 cells as a way to mark polyubiquitinated protein. A potent inhibitor of the proteasome, MG132, was shown to block clearance of the polyubiquitinated protein whereas this effect was not evident following Nelfinavir treatment (figure 3.12). This suggests that the effect of Nelfinavir on enhancing autophagy is probably not due to proteasomal inhibition alone. There does not appear to be any inhibitory effects of Nelfinavir on the proteasome at this 4 h time point. Due to the lack of sensitivity of this assay, there is a possibility that there might be a very small level of inhibition of the proteasome.

Figure 3.12

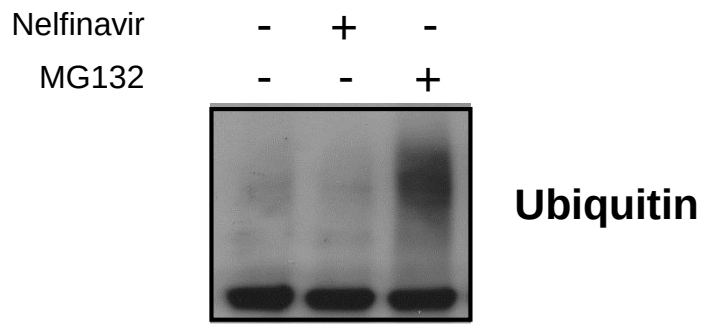

Figure 3.12. The increases in autophagy caused by Nelfinavir are not due to proteasomal inhibition alone. *HEK 293 cells were transfected with a vector expressing a polyubiquitinated protein and treated with either Nelfinavir (30μM) or MG132 (10 mM) for 4 h. An accumulation of the polyubiquitinated protein was not observed in the Nelfinavir treatment condition suggesting the proteasome was not inhibited.*

3.11 Nelfinavir's effects are dominant to Chloroquine

The findings to this point led to the hypothesis that a potential therapeutic strategy for diseases with dysfunctional mTORC1 activity would be to treat cells with both the ER stress inducing drug Nelfinavir in combination with an inhibitor of autophagy. This treatment would hypothetically differentially effect cells with high/constitutively active mTORC1 signalling and wild-type cells with normal levels of mTORC1 activity due to different basal levels of ER stress. It was thought that this combination treatment, at the correct concentrations, would moderately stress wild-type cells and thus only induce cell survival mechanisms but stress the mutant cells with high mTORC1 signalling to a greater degree. The expectation was that mTORC1 active cells would not tolerate this drug combination of ER stress and autophagy inhibition and thus induce apoptotic events.

A known inhibitor of autophagy, Chloroquine, was used to test this strategy given its status as a clinically approved and viable drug used in the treatment of malaria in humans. Following a number of combination treatments at varying concentrations, western blotting indicated that the levels of autophagy induction and inhibition of mTORC1 signalling were not restored by Chloroquine suggesting that the effects of Nelfinavir on cells is dominant (figure 3.13). Bafilomycin A1, another autophagy inhibitor was also employed as a positive control.

It should be noted that in figure 3.11, Nelfinavir was causing accumulation of LC3-II whereas this was not observed in figure 3.13. It may be that at shorter time points (such as 4 hours in figure 3.13) Nelfinavir is driving autophagy but at later time points (such as 24 hours in figure 3.11), it may be having a similar effect to Thapsigargin and is perturbing autophagosome-lysosome fusion. This would account for the differing observations of LC3-II accumulation and also the observation of numerous small intracellular entities seen in Nelfinavir treated cells (observed via microscopy and discussed later), which could be autophagosomes that have accumulated.

Figure 3.13

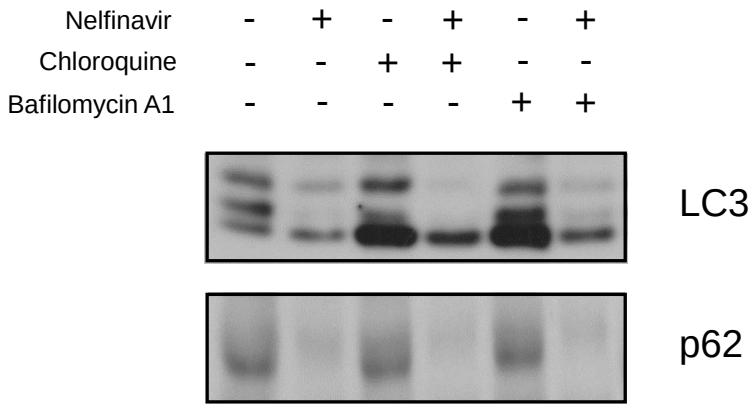

Figure 3.13. Nelfinavirs activation of autophagy is dominant to the inhibitory effects of Chloroquine and Bafilomycin A1. *HEK293 cells were treated with combinations of Nelfinavir (30 µM), Chloroquine (50 µM) and Bafilomycin A1 (2.5 nM) (another inhibitor of autophagy) for 4 h. Levels of p62 and the proportion of the lower lapidated isoform of LC3 (LC3-II) in the combination treatment conditions resembled that of the Nelfinavir only condition, suggesting Nelfinavir's effects were dominant.*

3.12 Chloroquine enhances cell death induced by Nelfinavir

The effects of the combination treatment were then observed through microscopy of ELT3 cells, another cellular model of TSC, that have either loss of TSC2 (ELT3-V3) or TSC2 re-expressed (ELT3-T3) (figure 3.14). This strategy allowed for the preliminary qualitative assessment of cell death by bright field microscopy. Minimal reduction in cell numbers or evidence of apoptotic cells was observed in those cells treated with Chloroquine alone, in both ELT3 cell lines without TSC2 or cells re-expressing TSC2. A reduction in cell numbers and increased evidence of cell death was observed in the Nelfinavir treatment conditions and these effects were more pronounced as concentrations of Nelfinavir was increased. In the combination treatment with both Nelfinavir and Chloroquine, the effects of Nelfinavir were greatly increased and suggests that Chloroquine was having an additive

effect. Most importantly to note, was that these drug effects were significantly greater in the ELT3-V3 cells that lack TSC2 compared to the TSC2 expressing rescue cells. Such findings demonstrate that this combination treatment was acting selectively.

Figure 3.14

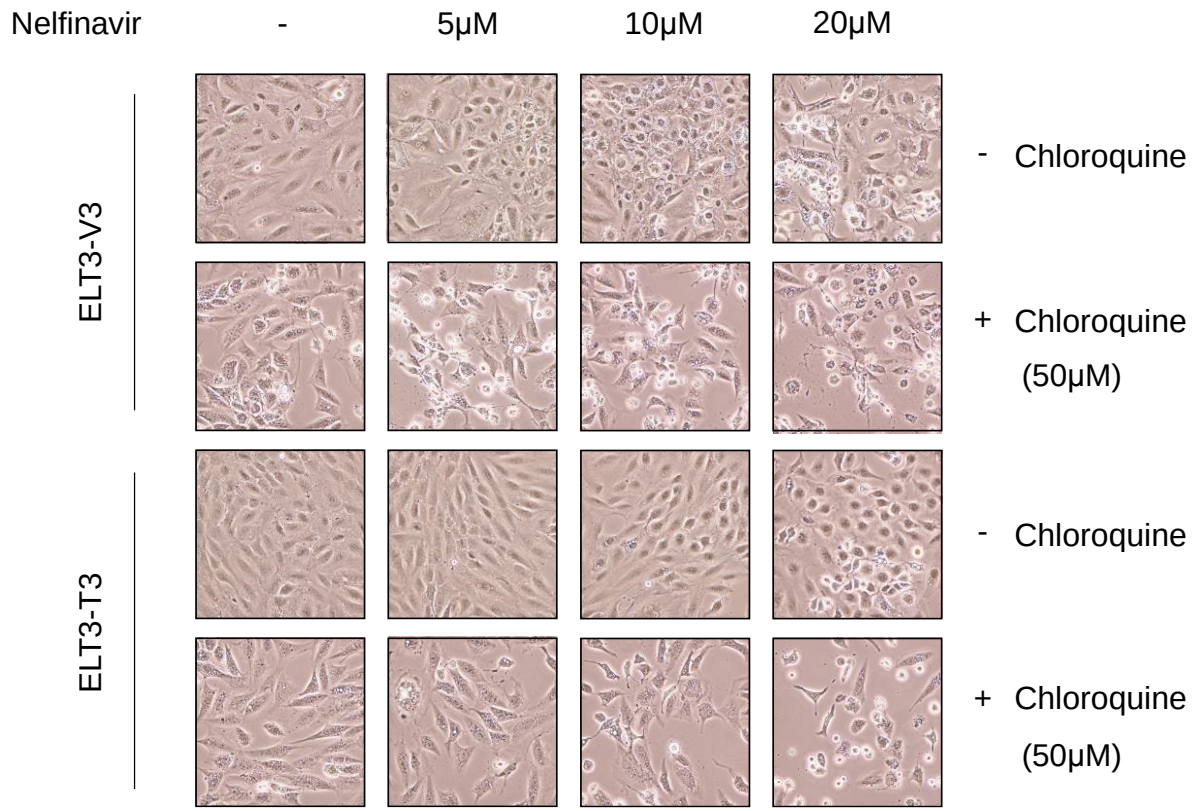

Figure 3.14. Enhanced cell death observed in cells lacking TSC2 following Nelfinavir and Chloroquine treatment*. ELT3 cells were treated for 24 h at the drug concentrations indicated (5, 10 & 20 μM Nelfinavir and 50 μM Chloroquine) and then visualised using bright field microscopy. Apparent increased cell death was observed as Nelfinavir concentration increased and the greatest amount of cell death was observed in the combination treatment conditions. Most importantly, the effects were greater in the TSC2 null cells relative to the TSC2$^{+/+}$ cells showing that this treatment strategy operates selectively.*

3.13 Nelfinavir and chloroquine dramatically and selectively induce cell death in TSC deficient cells

The final stage of experimentation sought to quantify the levels of cell death, as observed previously through microscopy. Firstly, cyquant cellular proliferation assays were undertaken and this allowed for the quantification of cell numbers in different treatment conditions. The difference in cell number relative to control could then be determined and this difference would represent the extent of cell death that had been induced by the treatments. The results of these assays on TSC2 cells mirrored the microscopy observations of the ELT3 cells in that Nelfinavir increased cell death in the *TSC2* null cells (shown through a significant reduction in cell number) in the single drug treatment condition. The differences between the levels of cellular death observed in the *TSC2+/+* cells compared to the *TSC2-/-* cells was slight. In the combination treatment condition, however, the reduction in cell numbers (and inferred levels of cell death induction) was considerably higher and the differences between the *TSC2+/+* and *TSC-/-* cells were more significantly pronounced (figure 3.15).

Figure 3.15

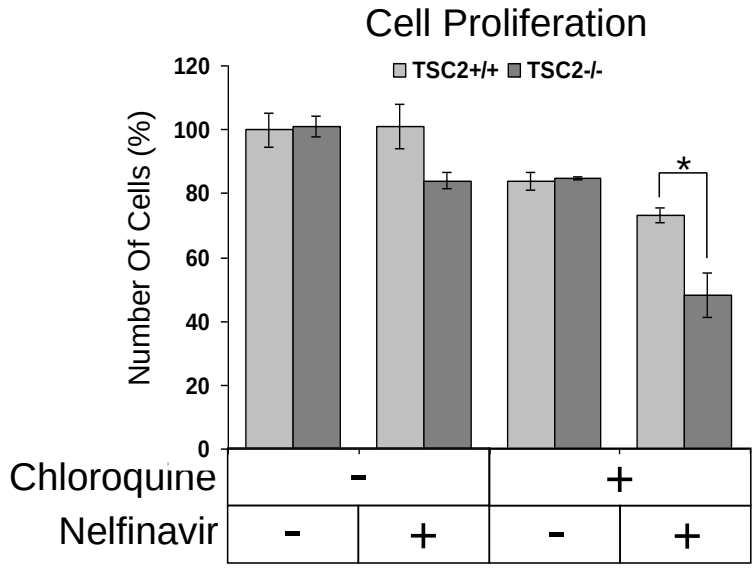

Figure 3.15 Nelfinavir and Chloroquine significantly and selectively reduce cell number in TSC2-deficient cells. *TSC2 $^{+/+}$ and TSC2 $^{-/-}$ MEFS were treated with combinations of Nelfinavir (30 µM) and Chloroquine (25 µM) for 24 h. Cyquant cellular proliferation assays indicated a significant reduction in cell number in the Nelfinavir and Chloroquine combination treatments.*

Cell death ELISAs were then performed to reinforce the observations of the cell proliferation assays. The results of the ELISAs reiterated what was observed previously, in that some cell death was observed in both single drug treatments of Nelfinavir and Chloroquine. The most significant levels of cell death were observed in the combination treatment and it was in this condition that there was the greatest difference in the level of cell death between *TSC2+/+* and *TSC2-/-* cells (figure 3.16). It should be noted that this assay does not distinguish between necrosis and apoptosis. In future, further experimentation should be undertaken such as caspase cleavage assays to confirm the type of cell death that is being observed.

Figure 3.16

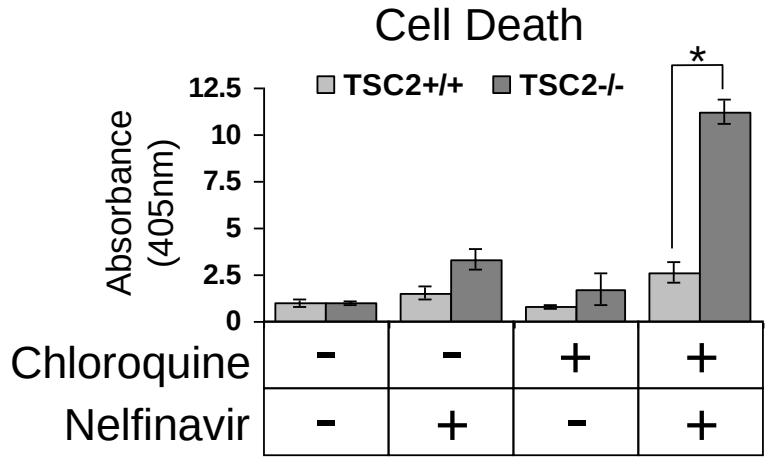

Figure 3.16. Nelfinavir and Chloroquine significantly and selectively induce cell death in TSC2-deficient cells. *TSC2 $^{+/+}$ and TSC2 $^{-/-}$ MEFS were treated with combinations of Nelfinavir (30 µM) and Chloroquine (25 µM) for 24 h. Cell Death ELISAs showed that the highest amount of cell death occurred in the combination treatment condition. By comparing results to the controls and solo treatment conditions, it is evident that combined treatment with both Nelfinavir and Chloroquine induces significant and selective cell death in TSC2 null cells.*

Figure 3.17

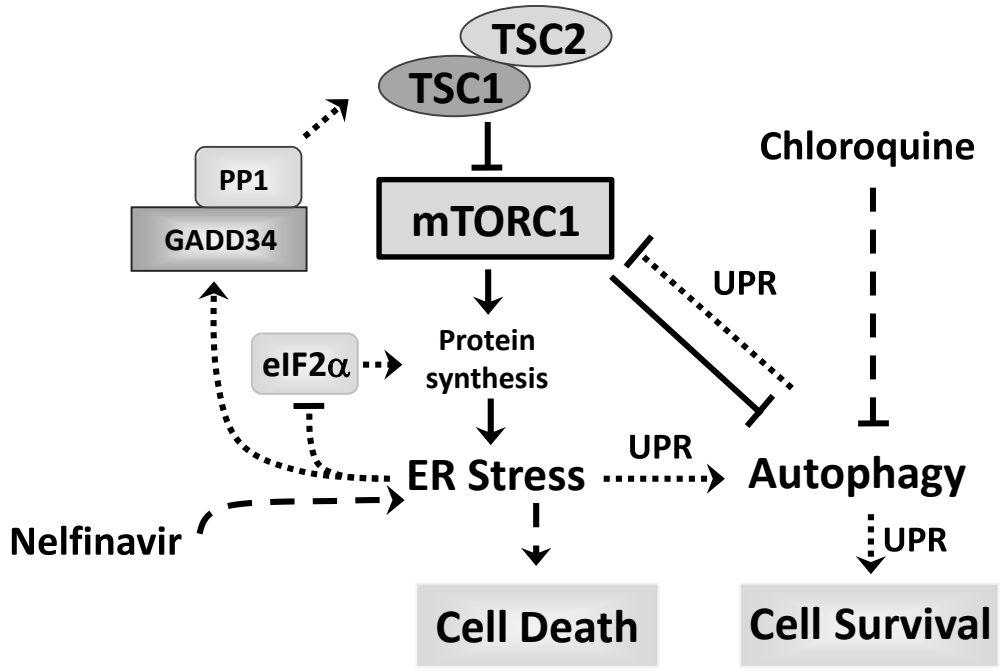

Figure 3.17 Diagram of the crosstalk and interactions between various signalling pathways. *Illustration of the molecular interactions between Nelfinavir, Chloroquine and the various signalling pathways. Nelfinavir is shown to target and enhance ER stress which, in combination with autophagy inhibition by Chloroquine, induces cell death.*

4. Discussion

The primary aim of this investigation was to examine whether it was possible to utilise the clinically viable drug Nelfinavir to specifically induce cell death in cells exhibiting aberrant mTOR activity. This investigation was able to successfully show that Nelfinavir was capable of inducing ER stress and subsequently cell death in *TSC2* null cells and this effect was selective in that the results were more pronounced compared to cells expressing wild type TSC2. It was however observed that many of the cells, both mutant and wild type, were able to survive following Nelfinavir treatment inferring that some form of cell survival mechanism was being exploited. It was found that upon treatment of Nelfinavir, autophagy was induced. This is one of the major events in the unfolded protein response and is a mechanism by which cells attempt to restore normal cellular protein levels and homeostasis. It appeared that *TSC2* null cells were heavily reliant on this survival pathway in order to withstand the effects of Nelfinavir and avoid the cell death inducing features of the ER stress response. Another mechanism that is employed by cells to restore protein homeostasis and which occurs prior to the aggregation of unfolded/misfolded proteins is via the proteasome (Rubinsztein, 2006). Previous research has indicated that Nelfinavir acts to inhibit the proteasome and this would account for its ability to induce ER Stress and observed elevations in autophagy levels (Bono et al, 2012; Gupta et al, 2007).

Given these findings, it was hypothesised that an inhibitor of autophagy in combination with Nelfinavir might further enhance cell death in *TSC2* null cells. The drug selected for use was Chloroquine, a drug already approved for clinical use in the treatment of malaria, which raises lysosomal pH and inhibits lysosomal protein degradation and autophagy. It was shown that through inhibiting autophagy with Chloroquine, *TSC2* null cells became vulnerable to Nelfinavir-induced cell death whereas wild type *TSC2* cells were able to tolerate the drug combination and survive. This demonstrates that these two drugs operate synergistically to significantly and selectively induce cell death in *TSC2* null cells. Furthermore, this therapeutic strategy of ER stress induction combined with autophagy inhibition has previously been shown to induce cell death in breast cancer as well as

other *TSC* deficient cell models (Parkhitko et al, 2011; Thomas et al, 2012). This suggests that this strategy of targeting both ER stress and autophagy may be more broadly applicable for a wider range of cancers and diseases.

This research highlights the importance that TSC2 has in a normal ER stress response. The sensitivity of the *TSC2* null cells to Nelfinavir is likely caused in part by the inability of these *TSC2* null cells to fully inhibit mTORC1. Inhibition of mTORC1 through TSC2 appears necessary to reduce ER stress, i.e., the rate of protein synthesis would be reduced that would consequently limit further stress of the ER from newly generated protein. The inhibition of mTORC1 is also required for a more potent autophagy response (via ULK1 activation) to effectively remove unfolded protein aggregates in the ER.

Direct interactions between TSC2 and the ER stress pathway have previously been described. The ER stress regulatory protein CHOP (aka GADD34), has been shown to recruit Protein Phosphatase 1 (PP1) to TSC2 which activates it through de-phosphorylation (Uddin et al, 2011; Watanabe et al, 2007; Kojima et al, 2003) and subsequently mTORC1 is inhibited. Difficulties were experienced in measuring later markers of the ER stress response such as CHOP protein during research despite cell death being apparent. The difficulties I observed with detecting CHOP protein was also observed from other groups where they also revealed that cells lacking TSC2 have a truncated ER stress response (Kang et al, 2011).

In addition to the work assessing the effectiveness of drug treatments, another aspect of this study was to examine interactions between mTORC1 signalling and ULK1, a major component of the autophagy pathway. Experiments demonstrated that ULK1 had a potent inhibitory effect on mTORC1 signalling shown through marked reduction in mTORC1 activity, as observed through phosphorylation of rpS6 and S6K1 when ULK1 is overexpressed. As evidenced by an upward Raptor mobility shift when resolved by SDS-PAGE, this inhibition of mTORC1 was due to Raptor phosphorylation by ULK1. ULK1 knockdown experiments by shRNA confirmed that ULK1 phosphorylated Raptor, and was a negative regulator of mTORC1 signal transduction. Interestingly,

Raptor mobility shifts were also observed when ULK2, another member of the Ulk protein family, was overexpressed suggesting some level of functional redundancy between both ULK1 and ULK2. Subsequent work has validated these observations and these ULK1-mediated phosphorylation events, which have been characterised. It was shown that ULK1 causes phosphorylation of Raptor at multiple sites. In particular, Ser855 and Ser859 residues of Raptor were strongly phosphorylated whilst Ser792 was moderately phosphorylated by ULK1. Functional work identified that ULK1 did not alter protein-protein interactions of mTORC1 components; while ULK1 phosphorylation of Raptor instead hindered binding of the substrate 4E-BP1 to Raptor. Overall, this research demonstrates ULK1's ability to inhibit mTORC1 signalling occurs via interference of substrate docking to Raptor (Dunlop et al, 2011).

In addition to the regulation of mTORC1 by ULK1, this study also observed that mTORC1 had an inhibitory effect on ULK1. Through the use of kinase assays, ULK1 activity was shown to be significantly reduced following insulin stimulation. This reduction was markedly lessened by the mTORC1 inhibitor, rapamycin. These findings highlight that homeostatic signalling interplay exists between mTORC1 and ULK1, which would switch depending on nutrient and energy status of the cell.

Although the effects of ULK1 on Raptor were shown to be independent of AMPK signalling in this study, other research has shown this signalling pathway to impact significantly both on autophagy and mTORC1; perhaps unsurprisingly given mTORC1's critical role in energy sensing. Research in HeLa cells demonstrated that similarly to observations seen in yeast, AMPK signalling directly influences autophagy in that when it is AMPK is inhibited, so too is autophagy (Meley et al, 2006). It has also been demonstrated that AMPK regulates mTORC1 activity through phosphorylation of TSC2 and also through phosphorylation of Raptor (Inoki et al, 2003). Therefore, a complex pathway involving crosstalk and feedback exists between these three critical kinases, mTORC1, AMPK, and ULK1.

In conclusion, this study has allowed for the identification of novel signalling mechanisms between mTORC1 and autophagy. It has also enabled us to ascertain that combinatorial therapies which function to induce or exacerbate ER stress and simultaneously inhibit autophagy are capable of selectively inducing cell death in cells with aberrant mTORC1 signalling.

In the future, this research should be advanced through pre-clinical work to test whether the combination of Nelfinvavir and Chloroquine has benefits in TSC mouse models or other cancer models with heightened mTORC1 signalling. Should these pre-clinical trials prove to be similarly successful in the murine models as was observed in the cell lines of this study, the next stage would be to trial the combination treatment in humans. As both Nelfinavir and Chloroquine are clinically approved and commonly used agents in humans, maximum tolerated doses have already been established and this should expedite the trial process. Patients with Tuberous Sclerosis or patients with sporadic cancers whose cancer genotype features mutations in *TSC1* or *TSC2* resulting in upregulated mTORC1 signalling would be ideal preliminary candidates for such a trial. If successful, the trials could be expanded to patients with other heritable mTORC1 associated disorders such as Neurofibromatosis (which occurs as a result of mutations in the *NF1* gene) or Burt Hogg Dubé Syndrome (which occurs as a result of mutations in the gene encoding Folliculin).

A further avenue of research could be to investigate alternative combinations of drugs that target ER stress and autophagy. As targeting ER stress and autophagy in combination has been shown to be an effective therapeutic strategy for cells with aberrant mTORC1 activity, the experiments undertaken as described could be reproduced but using alternative clinically viable drugs that target the same pathways but perhaps via different mechanisms. An example could be to use Bortezomib, a clinically approved drug commonly used in chemotherapy that induces ER stress via inhibition of the 26S proteasome, in place of Nelfinavir (Vaeteewoottacharn et al, 2013). The availability of alternative drugs that inhibit autophagy and that are clinically viable is considerably more limited compared to viable ER stress inducers. One clinically viable alternative that has been shown to have promise as an inhibitor of autophagy is Lucanthone, a drug already used in

chemotherapy, and so perhaps this could be investigated as a replacement for Chloroquine (Carew et al, 2011). By undertaking these experiments using a variety of different viable agents, the combination which results in the highest level of cell death induction in mutant cells and lowest level of cell death in wild type cells could be identified (i.e., the greatest difference in levels of cell death between mutant and wild type cells and therefore the most selective treatment). In addition to identifying the combination treatment with the greatest effectiveness in terms of selectivity, these experiments would also allow for cost-benefit analysis to be assessed by taking into account the toxicity profiles of the drugs used. This way the optimal treatment with the least intrusive or minimal side effect profile could be selected.

The final potential avenue for future research would be to investigate lipid metabolism in cells with aberrant mTORC1 activity. During this study, it was observed via microscopy that following the treatments with Nelfivavir, numerous small intracellular entities became evident within the mutant cells. As suggested previously in the results section, these may be autophagosomes. Alternatively, these could be lipid accumulations, an assumption that would appear sensible given that research has demonstrated that ER stress perturbs lipid metabolism (Fang et al, 2013). Given the observation that there appears to be differences in lipid metabolism in cells with aberrant mTORC1 activity compared to wild type cells following Nelfinavir treatment, this may present another pathway that could be exploited in a selective treatment strategy.

5. Bibliography

1. F. A. Agarraberes, S. R. Terlecky, J. F. Dice, An intralysosomal hsp70 is required for a selective pathway of lysosomal protein degradation. *J Cell Biol* **137**, 825-834 (1997).

2. M. Bach, M. Larance, D. E. James, G. Ramm, The serine/threonine kinase ULK1 is a target of multiple phosphorylation events. *Biochem J* **440**, 283-291 (2011).

3. E. Bejarano, A. M. Cuervo, Chaperone-mediated autophagy. *Proc Am Thorac Soc* **7**, 29-39 (2010).

4. D. M. Benbrook, A. Long, Integration of autophagy, proteasomal degradation, unfolded protein response and apoptosis. *Exp Oncol* **34**, 286-297 (2012).

5. C. Bono, L. Karlin, S. Harel, E. Mouly, S. Labaume, L. Galicier, S. Apcher, H. Sauvageon, J. P. Fermand, J. C. Bories, B. Arnulf, The human immunodeficiency virus-1 protease inhibitor nelfinavir impairs proteasome activity and inhibits the proliferation of multiple myeloma cells in vitro and in vivo. *Haematologica* **97**, 1101-1109 (2012).

6. J. S. Carew, C. M. Espitia, J. A. Esquivel, 2nd, D. Mahalingam, K. R. Kelly, G. Reddy, F. J. Giles, S. T. Nawrocki, Lucanthone is a novel inhibitor of autophagy that induces cathepsin D-mediated apoptosis. *J Biol Chem* **286**, 6602-6613 (2011).

7. H. Y. Cho, S. Thomas, E. B. Golden, K. J. Gaffney, F. M. Hofman, T. C. Chen, S. G. Louie, N. A. Petasis, A. H. Schonthal, Enhanced killing of chemo-resistant breast cancer cells via controlled aggravation of ER stress. *Cancer Lett* **282**, 87-97 (2009).

8. A. M. Cuervo, Autophagy: many paths to the same end. *Mol Cell Biochem* **263**, 55-72 (2004).

9. S. Di Bartolomeo, M. Corazzari, F. Nazio, S. Oliverio, G. Lisi, M. Antonioli, V. Pagliarini, S. Matteoni, C. Fuoco, L. Giunta, M. D'Amelio, R. Nardacci, A. Romagnoli, M. Piacentini, F. Cecconi, G. M.

Fimia, The dynamic interaction of AMBRA1 with the dynein motor complex regulates mammalian autophagy. *J Cell Biol* **191**, 155-168 (2010).

10. J. F. Dice, H. L. Chiang, E. P. Spencer, J. M. Backer, Regulation of catabolism of microinjected ribonuclease A. Identification of residues 7-11 as the essential pentapeptide. *J Biol Chem* **261**, 6853-6859 (1986).

11. E. A. Dunlop, D. K. Hunt, H. A. Acosta-Jaquez, D. C. Fingar, A. R. Tee, ULK1 inhibits mTORC1 signaling, promotes multisite Raptor phosphorylation and hinders substrate binding. *Autophagy* **7**, 737-747 (2011).

12. E. A. Dunlop, A. R. Tee, Mammalian target of rapamycin complex 1: signalling inputs, substrates and feedback mechanisms. *Cell Signal* **21**, 827-835 (2009).

13. D. Egan, J. Kim, R. J. Shaw, K. L. Guan, The autophagy initiating kinase ULK1 is regulated via opposing phosphorylation by AMPK and mTOR. *Autophagy* **7**, 643-644 (2011).

14. D. L. Fang, Y. Wan, W. Shen, J. Cao, Z. X. Sun, H. H. Yu, Q. Zhang, W. H. Cheng, J. Chen, B. Ning, Endoplasmic reticulum stress leads to lipid accumulation through upregulation of SREBP-1c in normal hepatic and hepatoma cells. *Mol Cell Biochem* **381**, 127-137 (2013).

15. D. C. Fingar, C. J. Richardson, A. R. Tee, L. Cheatham, C. Tsou, J. Blenis, mTOR controls cell cycle progression through its cell growth effectors S6K1 and 4E-BP1/eukaryotic translation initiation factor 4E. *Mol Cell Biol* **24**, 200-216 (2004).

16. D. C. Fingar, S. Salama, C. Tsou, E. Harlow, J. Blenis, Mammalian cell size is controlled by mTOR and its downstream targets S6K1 and 4EBP1/eIF4E. *Genes Dev* **16**, 1472-1487 (2002).

17. J. J. Gills, J. Lopiccolo, J. Tsurutani, R. H. Shoemaker, C. J. Best, M. S. Abu-Asab, J. Borojerdi, N. A. Warfel, E. R. Gardner, M. Danish, M. C. Hollander, S. Kawabata, M. Tsokos, W. D. Figg, P. S.

Steeg, P. A. Dennis, Nelfinavir, A lead HIV protease inhibitor, is a broad-spectrum, anticancer agent that induces endoplasmic reticulum stress, autophagy, and apoptosis in vitro and in vivo. *Clin Cancer Res* **13**, 5183-5194 (2007).

18. A. K. Gupta, B. Li, G. J. Cerniglia, M. S. Ahmed, S. M. Hahn, A. Maity, The HIV protease inhibitor nelfinavir downregulates Akt phosphorylation by inhibiting proteasomal activity and inducing the unfolded protein response. *Neoplasia* **9**, 271-278 (2007).

19. D. M. Gwinn, D. B. Shackelford, D. F. Egan, M. M. Mihaylova, A. Mery, D. S. Vasquez, B. E. Turk, R. J. Shaw, AMPK phosphorylation of raptor mediates a metabolic checkpoint. *Mol Cell* **30**, 214-226 (2008).

20. C. He, D. J. Klionsky, Regulation mechanisms and signaling pathways of autophagy. *Annu Rev Genet* **43**, 67-93 (2009).

21. S. J. Healy, A. M. Gorman, P. Mousavi-Shafaei, S. Gupta, A. Samali, Targeting the endoplasmic reticulum-stress response as an anticancer strategy. *Eur J Pharmacol* **625**, 234-246 (2009).

22. M. K. Holz, B. A. Ballif, S. P. Gygi, J. Blenis, mTOR and S6K1 mediate assembly of the translation preinitiation complex through dynamic protein interchange and ordered phosphorylation events. *Cell* **123**, 569-580 (2005).

23. T. Hosoi, A. Kume, K. Otani, T. Oba, K. Ozawa, A unique modulator of endoplasmic reticulum stress-signalling pathways: the novel pharmacological properties of amiloride in glial cells. *Br J Pharmacol* **159**, 428-437 (2010).

24. R.C. Hresko, M. Mueckler. mTOR.RICTOR is the Ser473 kinase for Akt/protein kinase B in 3T3-L1 adipocytes. *J Biol Chem* **280**, 40406-16 (2005).

25. K .H .Huang, K. L. Kuo , I. L. Ho, H. C. Chang, Y. T. Chuang, W. C. Lin, P. Y. Lee, S.C. Chang, C. K. Chiang, Y.S. Pu, C. T. Chou, C. H. Hsu, S. H. Liu. Celecoxib-induced cytotoxic effect is potentiated by inhibition of autophagy in human urothelial carcinoma cells. *PLoS One* **8**,e82034 (2013).

26. K. Inoki, T. Zhu, K. L. Guan, TSC2 mediates cellular energy response to control cell growth and survival. *Cell* **115**, 577-590 (2003).

27. Y. J. Kang, M. K. Lu, K. L. Guan, The TSC1 and TSC2 tumor suppressors are required for proper ER stress response and protect cells from ER stress-induced apoptosis. *Cell Death Differ* **18**, 133-144 (2011).

28. J. Kim, M. Kundu, B. Viollet, K. L. Guan, AMPK and mTOR regulate autophagy through direct phosphorylation of Ulk1. *Nat Cell Biol* **13**, 132-141 (2011).

29. M. A. Knowles, T. Habuchi, W. Kennedy, D. Cuthbert-Heavens, Mutation spectrum of the 9q34 tuberous sclerosis gene TSC1 in transitional cell carcinoma of the bladder. *Cancer Res* **63**, 7652-7656 (2003).

30. M. A. Knowles, F. M. Platt, R. L. Ross, C. D. Hurst, Phosphatidylinositol 3-kinase (PI3K) pathway activation in bladder cancer. *Cancer Metastasis Rev* **28**, 305-316 (2009).

31. E. Kojima, A. Takeuchi, M. Haneda, A. Yagi, T. Hasegawa, K. Yamaki, K. Takeda, S. Akira, K. Shimokata, K. Isobe, The function of GADD34 is a recovery from a shutoff of protein synthesis induced by ER stress: elucidation by GADD34-deficient mice. *Faseb j* **17**, 1573-1575 (2003).

32. M. Kraus, J. Bader, H. Overkleeft, C. Driessen, Nelfinavir augments proteasome inhibition by bortezomib in myeloma cells and overcomes bortezomib and carfilzomib resistance. *Blood Cancer J* **3**, e103 (2013).

33. M. Laplante, D. M. Sabatini, mTOR signaling at a glance. *J Cell Sci* **122**, 3589-3594 (2009).

34. J. W. Lee, S. Park, Y. Takahashi, H. G. Wang, The association of AMPK with ULK1 regulates autophagy. *PLoS One* **5**, e15394 (2010).

35. W. W. Li, J. Li, J. K. Bao, Microautophagy: lesser-known self-eating. *Cell Mol Life Sci* **69**, 1125-1136 (2012).

36. W. Li, Q. Yang, Z. Mao, Chaperone-mediated autophagy: machinery, regulation and biological consequences. *Cell Mol Life Sci* **68**, 749-763 (2011).

37. A. S. Loffler, S. Alers, A. M. Dieterle, H. Keppeler, M. Franz-Wachtel, M. Kundu, D. G. Campbell, S. Wesselborg, D. R. Alessi, B. Stork, Ulk1-mediated phosphorylation of AMPK constitutes a negative regulatory feedback loop. *Autophagy* **7**, 696-706 (2011).

38. D. Meley, C. Bauvy, J. H. Houben-Weerts, P. F. Dubbelhuis, M. T. Helmond, P. Codogno, A. J. Meijer, AMP-activated protein kinase and the regulation of autophagic proteolysis. *J Biol Chem* **281**, 34870-34879 (2006).

39. O. Muller, T. Sattler, M. Flotenmeyer, H. Schwarz, H. Plattner, A. Mayer, Autophagic tubes: vacuolar invaginations involved in lateral membrane sorting and inverse vesicle budding. *J Cell Biol* **151**, 519-528 (2000).

40. D. A. Nijholt, T. R. de Graaf, E. S. van Haastert, A. O. Oliveira, C. R. Berkers, R. Zwart, H. Ovaa, F. Baas, J. J. Hoozemans, W. Scheper, Endoplasmic reticulum stress activates autophagy but

not the proteasome in neuronal cells: implications for Alzheimer's disease. *Cell Death Differ* **18**, 1071-1081 (2011).

41. U. Ozcan, L. Ozcan, E. Yilmaz, K. Duvel, M. Sahin, B. D. Manning, G. S. Hotamisligil, Loss of the tuberous sclerosis complex tumor suppressors triggers the unfolded protein response to regulate insulin signaling and apoptosis. *Mol Cell* **29**, 541-551 (2008).

42. A. Parkhitko, F. Myachina, T. A. Morrison, K. M. Hindi, N. Auricchio, M. Karbowniczek, J. J. Wu, T. Finkel, D. J. Kwiatkowski, J. J. Yu, E. P. Henske, Tumorigenesis in tuberous sclerosis complex is autophagy and p62/sequestosome 1 (SQSTM1)-dependent. *Proc Natl Acad Sci U S A* **108**, 12455-12460 (2011).

43. F. M. Platt, C. D. Hurst, C. F. Taylor, W. M. Gregory, P. Harnden, M. A. Knowles, Spectrum of phosphatidylinositol 3-kinase pathway gene alterations in bladder cancer. *Clin Cancer Res* **15**, 6008-6017 (2009).

44. M. T. Rosenfeldt, K. M. Ryan, The multiple roles of autophagy in cancer. *Carcinogenesis* **32**, 955-963 (2011).

45. D. C. Rubinsztein, The roles of intracellular protein-degradation pathways in neurodegeneration. *Nature* **443**, 780-786 (2006).

46. J. R. Sampson, Therapeutic targeting of mTOR in tuberous sclerosis. *Biochem Soc Trans* **37**, 259-264 (2009).

47. A. Saito, K. Ochiai, S. Kondo, K. Tsumagari, T. Murakami, D. R. Cavener, K. Imaizumi. Endoplasmic reticulum stress response mediated by the PERK-eIF2(alpha)-ATF4 pathway is involved in osteoblast differentiation induced by BMP2. *J Biol Chem* **286**, 4809-18 (2011).

48. S. Thomas, N. Sharma, E. B. Golden, H. Cho, P. Agarwal, K. J. Gaffney, N. A. Petasis, T. C. Chen, F. M. Hofman, S. G. Louie, A. H. Schonthal, Preferential killing of triple-negative breast cancer cells in vitro and in vivo when pharmacological aggravators of endoplasmic reticulum stress are combined with autophagy inhibitors. *Cancer Lett* **325**, 63-71 (2012).

49. M. N. Uddin, S. Ito, N. Nishio, T. Suganya, K. Isobe, Gadd34 induces autophagy through the suppression of the mTOR pathway during starvation. *Biochem Biophys Res Commun* **407**, 692-698 (2011).

50. K. Vaeteewoottacharn, R. Kariya, K. Matsuda, M. Taura, C. Wongkham, S. Wongkham, S. Okada, Perturbation of proteasome function by bortezomib leading to ER stress-induced apoptotic cell death in cholangiocarcinoma. *J Cancer Res Clin Oncol* **139**, 1551-1562 (2013).

51. R. Watanabe, Y. Tambe, H. Inoue, T. Isono, M. Haneda, K. Isobe, T. Kobayashi, O. Hino, H. Okabe, T. Chano, GADD34 inhibits mammalian target of rapamycin signaling via tuberous sclerosis complex and controls cell survival under bioenergetic stress. *Int J Mol Med* **19**, 475-483 (2007).

52. Q. Yang, K. L. Guan, Expanding mTOR signaling. *Cell Res* **17**, 666-681 (2007).